

## Supporting Information

### **A Nuclear Targeting Two-Photon Absorption Iridium Complex Induced Dual-damage in Photon Dynamic Therapy: Localization Matters**

*Xiaohe Tian\**, *Yingzhong Zhu*, *Mingzhu Zhang*, *Lei Luo*, *Jieying Wu*, *Hongping Zhou*, *Lijuan Guan*, *Giuseppe Battaglia*, *Yupeng Tian\**

## Content

Materials and general instruments .....	1
The equation of the fluorescence quantum yields ( $\Phi$ ) .....	2
Determination of two photon absorption cross sections .....	2
Cytotoxicity assay .....	3
Fixed cell and inhibitors studies .....	3
TEM cell imaging .....	4
Animal method: .....	5
Image processing and analysis .....	5
Scheme S1. The synthetic routs for Ir complexes .....	6
Synthesis .....	6
Synthesis of complexes Ir0 .....	6
Synthesis of complex Ir-Es .....	6
Synthesis of complex Ir-Me .....	7
Synthesis of complex Ir-Pn .....	7
Synthesis of complex Ir-Pc .....	8
Synthesis of complex Ir-Cz .....	8
Synthesis of complex Ir(bpy) .....	9
Fig. S1. <sup>1</sup> H NMR spectra of the five Ir complexes (Ir-Es, Ir-Me, Ir-Pn, Ir-Pc, and Ir-Cz) in CD <sub>3</sub> CN .....	11
Fig. S2. The <sup>1</sup> H NMR spectrum of Ir-(bpy) .....	11
Fig. S3. ESI-MS spectra of the five Ir complexes (Ir-Es, Ir-Me, Ir-Pn, Ir-Pc, and Ir-Cz) .....	13
Fig. S4. The ESI-MS spectrum of Ir-(bpy) .....	13
Fig. S5. The crystal structure of complexes Ir-Me (H atoms, solvent molecules, and anion have been omitted for clarity; thermal ellipsoids are drawn at 50 % probability) .....	14
Table S1. Crystal data collection and structure refinement for Ir-Me .....	14
Fig. S6. The UV-vis absorption spectra (left) and luminescent spectra (right) of Ir complexes (Ir-Es, Ir-Me, Ir-Pn, Ir-Pc, and Ir-Cz) in dichloromethane ( $c = 1 \times 10^{-5}$ M) .....	15
Table S2. The photophysical properties of complexes Ir-Me and Ir-Es in dichloromethane .....	15
Fig. S7. Two-photon absorption cross sections of five Ir(III) complexes in dichloromethane with excited wavelength from 700 nm to 900 nm .....	15
Fig. S8. HepG2 cells toxicity data under dark and UV light condition (interval=6 hours, 5 minutes/time, concentration 10 $\mu$ M) for Ir-Pn, Ir-Pc, and Ir-Cz obtained from the MTT assay after incubated for 24 h. ....	16

Fig. S9. Normal cells HELF toxicity data results of Ir-Es, Ir-Me, Ir-Pn, Ir-Pc and Ir-Cz (c = 1, 10, 20 $\mu$ M) obtained from the MTT assays after incubation for 24 h. ....	16
Fig. S10. The decrease of absorption of ADPA (100 $\mu$ M in PBS mixed with 5 $\mu$ M Ir-Pn, Ir-Pc and Ir-Cz, respectively) with laser exposure for 1, 3, 5, 10, 15 min. ....	17
Fig. S11. Confocal micrographs (one-photon and two-photon) of HepG2 cells incubated with Ir-Es and Ir-Me complex (5 $\mu$ M). The scale bar represents 20 $\mu$ m. ....	17
Fig. S12. Confocal micrographs (one-photon and two-photon) of HepG2 cells incubated with Ir-Pn, Ir-Pc, and Ir-Cz (5 $\mu$ M). The scale bar represents 20 $\mu$ m. ....	18
Fig. S13. Single cell intensity profile of HepG2 cells uptake Ir-Es and Ir-Me complex. ....	18
Fig. S14. 3D fluorescence imaging photograph of live HepG2 cells incubated with 5 $\mu$ M Ir-Es for 30 min at 37 $^{\circ}$ C. ....	19
Fig. S15. Co-localization studies of Ir-Me with Mito-FR and DAPI. Insert: colocalization profile and Rr number showed the overlap coefficient. Scale bar = 10 $\mu$ m. ....	19
Fig. S16. The cell uptake inhibited experiment of Ir-Me and Ir-Es with six typical inhibitors. ....	20
Fig. S17. The cell entry inhibitors experiment of Ir-Pc treat with six typical inhibitors and low temperature experiment. Scale bar=5 $\mu$ m. ....	20
Fig. S18. The normalized cell uptake intensity from Fig. S17. ....	21
Fig. S19. Confocal microscopy imaging of fixed HepG2 cell incubated with Ir-Me and Ir-Es for 30 min. Scale bar = 10 $\mu$ m. ....	21
Fig. S20. TEM imaging of HepG2 cell incubated with Ir-Me without OsO <sub>4</sub> . Scale bar = 5 $\mu$ m. ....	21
Fig. S21. Ir-Me PDT effect in HepG2 cells. Scale bar = 10 $\mu$ m. ....	22
Fig. S22. The co-localization experiment using Ir-(bpy) complex and mitochondrial tracker Mitotracker Far-red. Scale bar= 5 $\mu$ m. ....	22
Fig. S23. The PDT experiment using Ir-(bpy) complex for continued 30-time scanning. ....	22
Fig. S24. DNA cleavage effect using Ir-Es complex under inhibition of <sup>1</sup> O <sub>2</sub> . ....	23
Fig. S25. PDT performance of Ir-Es complex under hypoxia condition; Scale bar=5 $\mu$ m. ....	23
Fig. S26. ICP-MS quantifications of Iridium (Ir-Es) in different subcellular organelles before and after UV irradiation. ....	24
Fig. S27. Confocal fluorescence images of JC-1 stained HepG2 cells pre-treated with Ir-Es and Ir-Me under different irradiation time. Scale bar = 10 $\mu$ m. ....	25
Fig. S28. Confocal fluorescence images of Annexin V-FITC/PI stained HepG2 cells pre-treated with Ir-Es and Ir-Me under different irradiation time. Scale bar = 10 $\mu$ m. ....	26
Fig. S29. TEM imaging of HepG2 cell incubated with Ir-Me with OsO <sub>4</sub> and treated under UV light (illumination = 30 s, interval = 30 min). Scale bar = 5 $\mu$ m. ....	26

Fig. S30. The fluorescence emission spectra of Ir-Es ( $2 \times 10^{-5}$ M) mixed with different bio-molecule (1, control; 2, CD-DNA; 3, PBR 322, 4, RNA; 5, L-Glutamic acid; 6, DL-Methionine; 7, Aspartic acid; 8, Leucine; 9, Tyrosine; 10, proline; 11, Tryptophan; 12, Serine; 13, L-Threonine).....	27
Fig. S31. The molecular docking models obtained from modeling the interaction between Ir-Es with DNA fragment. ....	27
Fig. S32. <i>In vivo</i> PDT extracted mouse solid tumor model after 21 <sup>st</sup> days, treated with PBS, 660 nm light only, Ir-Me complex, <i>Ce6</i> and Ir-Es complex. ....	28
Fig. S33. (a) Tumours at 21st days post-treatment and corresponding H&E staining of tumour slides. (b). Tumours at 21st days post-treatment and corresponding TUNEL staining of tumour slides. Scale bars = 100 $\mu$ m. ....	28
Reference: .....	29

## Materials and general instruments

All buffer components were of biological grade and were used as received. All chemical agents were commercial available and were used without further purification. Mitotracker<sup>®</sup> Far Red FM (MT-FR), and DAPI, trihydrochloride, trihydrate, fluoroPure<sup>™</sup> grade were purchased from Invitrogen. The complexes were dissolved in DMSO preceding the bio-experiments; then solutions of complexes were added to appropriate medium, which results a final DMSO concentration less than 1% (v/v).

Elemental analyses were performed with a perking Elmer240C elemental analyzer. <sup>1</sup>H NMR and <sup>13</sup>C NMR spectra were recorded on a Bruker Avance 400 spectrometer, and the chemical shifts are reported as parts per million from TMS ( $\delta$ ). Mass spectra were acquired on a Micromass GCT-MS (ESI source). UV-vis absorption spectra were recorded on a UV-265 spectrophotometer (concentration  $1 \times 10^{-5}$  M). Photoluminescence measurements were carried out on a Hitachi F-7000 fluorescence spectrophotometer (concentration  $5 \times 10^{-5}$  M) with a 450 W Xe lamp. Photoluminescence lifetime was studied on Horiba Fluoro Max-4P by using a LED lamp as the excitation source. The nonlinear optical properties were measured by the two-photon luminescence method with a femtosecond laser pulse and Ti:95 Sapphire System (680-1080 nm, 80 MHz, 140 fs, Chameleon II) as the light source. A 1 cm cell of the sample in dichloromethane at  $5.0 \times 10^{-4}$  mol L<sup>-1</sup> was put in the light path, and all measurement were carried out at room temperature.

The X-ray diffraction measurements were performed on a Bruker SMART CCD area detector using graphite monochromated Mo-K <sub>$\alpha$</sub>  radiation ( $\lambda = 0.710698$  Å) at 298(2) K. Intensity data were collected in the variable  $\omega$ -scan mode. The structures were solved by direct methods and difference Fourier syntheses. The non-hydrogen atoms were refined anisotropically and hydrogen atoms were introduced geometrically. Calculations were performed with a SHELXTL-97 program package.

Cells were recorded on a ZEISS LSM 710 META confocal laser-scanning microscope with a 40/63 oil lens. A Coherent Chameleon pulsed infrared multiphoton laser was used for two-photon imaging (760 nm). For real-time live cell imaging, the incubation chamber was connected to a ZEISS temperature control unit at 37 °C and a CO<sub>2</sub> controller with appropriate humidity (temperature and CO<sub>2</sub> concentration were allowed to stabilize for 1–2 hours before the experiment). For Ir complex, an excitation wavelength of 800 nm was used and the emission

was measured at 550–650 nm. Co-staining was performed by incubating the cells with 5  $\mu\text{M}$  Mitotracker Deep Red ( $\lambda_{\text{ex}} = 633 \text{ nm}$ ,  $\lambda_{\text{em}} = 650\text{--}680 \text{ nm}$ ) for 10 min and 5  $\mu\text{M}$  DAPI ( $\lambda_{\text{ex}} = 405 \text{ nm}$ ,  $\lambda_{\text{em}} = 420\text{--}450 \text{ nm}$ ) for 10 min. For transmission electron microscopy (TEM), HepG2 cells were incubated with Ir complexes (30 min) and then fixed by 3% glutaraldehyde and dehydrated by anhydrous ethanol. TEM samples were sectioned in Araldite resin using a microtome and examined on a FEI Tecnai instrument operating at 80 kV equipped with a Gatan 1k CCD camera. Imaging data acquisition and processing were performed using Zeiss LSM Image Browser, Zeiss LSM Image Expert and Image J.

### The equation of the fluorescence quantum yields ( $\Phi$ )

The fluorescence quantum yields ( $\Phi$ ) were determined by using  $[\text{Ru}(\text{bpy})_3]^{2+}$  ( $\Phi = 0.029$ ) as the reference according to the literature method [1, 2]. Quantum yields were corrected as follows:

$$\Phi_s = \Phi_r \frac{\int F_s A_r n_s^2}{\int F_r A_s n_r^2}$$

Where the  $s$  and  $r$  indices designate the sample and reference samples, respectively,  $A$  is the absorbance at  $\lambda_{\text{exc}}$ .  $n$  is the average refractive index of the appropriate solution.  $F$  is the integrated area under the corrected emission spectrum.  $\Phi$  is the quantum yield.

### Determination of two photon absorption cross sections

The two-photon absorption spectra of the probes are determined by two-photon induced luminescence method [3] by using Rhodamine B in ethanol as reference. The two-photon luminescence measurements were performed in fluorometric quartz cuvettes. The experimental luminescence excitation and detection conditions are conducted with negligible reabsorption processes, which can affect 2PA measurements. The two-photon absorption cross section of the probe is calculated at each wavelength according to the equation below:

$$\delta = \delta_{\text{ref}} \frac{\Phi_{\text{ref}}}{\Phi} \frac{C_{\text{ref}}}{C} \frac{n_{\text{ref}}}{n} \frac{F}{F_{\text{ref}}}$$

Here, the subscripts *ref* stands for the reference molecule.  $\delta$  is the 2PA cross-section value,  $c$  is the concentration of solution,  $n$  is the refractive index of the solution,  $F$  is the integrated area of

the detected two-photon-induced fluorescence signal, and  $\Phi$  is the fluorescence quantum yield. The  $\delta_{\text{ref}}$  value of reference is taken from the literature [4].

### **Cytotoxicity assay**

To determine the cytotoxic effect of Ir complexes which treated over 24h as a period, the 5-dimethylthiazol-2-yl-2,5-diphenyltetrazolium bromide (MTT) assay was performed. When HepG2 cells reached ~70 % confluence, HepG2 cells were harvested by trypsin and plated in flat-bottom 96-well plates for 24 h. Prior to the treatment of Ir complexes, the medium was removed and replaced with fresh medium/DMSO = 99/1 (containing concentration of Ir complexes 1, 5, 10, 15  $\mu\text{M}$ ). Subsequently, the treated cells were incubated for 24 h at 37 °C with 5%  $\text{CO}_2$ . After that, the cells were treated with 5 mg/mL MTT (40  $\mu\text{L}$ /well) and incubated for another 4 h (37 °C, 5%  $\text{CO}_2$ ). Then medium was removed, the formazan crystals were dissolved in DMSO(150  $\mu\text{L}$ /well), and the absorbance at 490 nm was recorded. The cell viability (%) was calculated according to the following equation: cell viability % =  $\text{OD}_{490}$  (sample)/ $\text{OD}_{490}$  (control)  $\times 100$ , where  $\text{OD}_{490}$  (sample) represented the optical density of the wells treated with various concentrations of the compounds and  $\text{OD}_{490}$  (control) represented that of the wells treated with DMEM + 10% FCS. Each concentration of Ir complexes covered eight wells which considered as one experimental group. And the averages and standard deviations were also reported. The reported percent of cell survival values are related to untreated control cells.

### **Fixed cell and inhibitors studies**

HepG2 cell was cultured in glass-bottom dish for 48 h, after that the cell was washed by PBS for 3 times and then incubated with 4% paraformaldehyde (1 mL). After that, the fixed cell was washed with PBS for 3 times and 5  $\mu\text{L}$  Ir complexes ( $1 \times 10^{-3}$  M in DMSO) was added to the plate and cultured for another 30 min (37 °C, 5%  $\text{CO}_2$ ). For inhibitors study, cells incubated with 1  $\mu\text{M}$  of inhibitors (including 2-deoxy-D-glucose,  $\text{NH}_4\text{Cl}$ , chloroquine, nocodazole, chlorpromazine, and colchicine, which dissolved in 1 mL culture medium without serum) for 30 min (37 °C, 5%  $\text{CO}_2$ ), then 5  $\mu\text{L}$  Ir complexes ( $1 \times 10^{-3}$  M in DMSO) was added to the plate and cultured for another 30 min (37 °C, 5%  $\text{CO}_2$ ). The imaging was carried out after the cells were washed by PBS for 3 times.

## Confocal cell imaging

Confocal microscopy imaging was acquired with a Carl Zeiss LSM 710 confocal microscopy and 63X/100X oil-immersion objective lens. The incubated cells were excited at 405 nm for Ir complexes for one-photon imaging, 633 nm for Mito-tracker Far Red, and 405 nm for DAPI with a semiconductor laser, and the emission signals were collected at  $580 \pm 20$  nm for Ir complexes,  $665 \pm 20$  nm for Mito-tracker Far Red, and  $430 \pm 20$  nm for DAPI, respectively. Two-photon confocal microscopy imaging of Ir complexes was excited at 800 nm and the emission signals were detected in the region of 580-620 nm. Quantization by line plots was accomplished by using the software package provided by Carl Zeiss instrument.

## TEM cell imaging

For TEM, HepG2 cells were incubated with **Ir-Me** and **Ir-Es** then fixed by using 3% glutaraldehyde and dehydrated with ethanol. For control cells and UV irradiation cells, secondary fixation was carried out in 1 % aqueous osmium tetroxide for 1 hour at room temperature, in order to visualize the membrane structures. For solely Iridium complex incubation group, the second fixation steps were ignored. The detailed protocols were listed as follow: For transmission electron microscopy, Cell specimens were received pelleted in Eppendorf tubes. Fresh 3 % glutaraldehyde in 0.1 M phosphate buffer was added to re-suspend the pellet to ensure optimal fixation, and left overnight at 4 °C. The specimens were then washed in 0.1 M-phosphate buffer at 4 °C, twice at 30 min intervals. Secondary fixation was carried out in 2 % aqueous osmium tetroxide for 2 hours at room temperature, followed by washing in buffer as above. Continuing at room temperature, this was followed by dehydration through a graded series of ethanol: 75% (15 min), 95% (15 min), 100% (15 min) and 100% (15 min). 100% ethanol was prepared by drying over anhydrous copper sulphate for 15min. The specimens were then placed in an intermediate solvent, propylene oxide, for two changes of 15mins duration. Resin infiltration was accomplished by placing the specimens in a 50/50 mixture of propylene oxide/Araldite resin. The specimens were left in this mixture overnight at room temperature. The specimens were left in full strength Araldite resin for 6-8 hrs at room temperature (with change of resin after 3-4 hrs) after which they were embedded in fresh Araldite resin for 48-72 hrs at 60 °C. Semi-thin sections approximately 0.5  $\mu\text{m}$  thick were cut on a Leica 10 ultramicrotome and stained with 1% Toluidine blue in Borax. Ultra-thin sections, approx. 70-90nm thick, were cut on a Leica ultramicrotome and stained for 25mins with saturated aqueous uranyl acetate followed by staining with Reynold's lead citrate for 5mins.

The sections were examined using a FEI Tecnai Transmission Electron Microscope at an accelerating voltage of 80kVv. Electron micrographs were taken using a Gatan digital camera.

### **Animal method:**

*All procedures involving animals were approved by and conformed to the guidelines of the Southwest University Animal Care Committee, College of Pharmaceutical Sciences. We have taken great efforts to reduce the number of animal used in these studies and also taken effort to reduce animal suffering from pain and discomfort.*

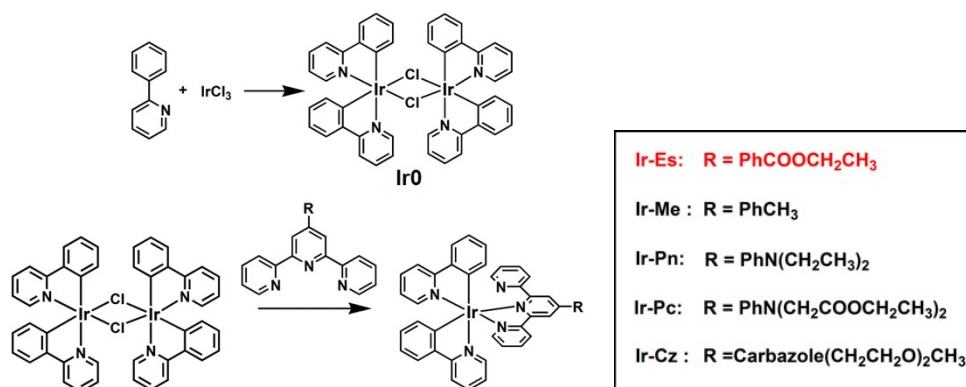
Chlorin e6 (Ce6) was purchased from Thermo Fisher Scientific. The 660 nm and 808 nm laser beam were obtained from Xian Midriver Optoelectronics Technology Co.

To develop murine breast cancer model, six to eight weeks old female BALB/c mice were subcutaneously injected at the right back with 0.1mL cell suspension containing  $5 \times 10^5$  4T1 cells. When the tumor size was 50-100 mm<sup>3</sup>, all the mice were randomly divided into six groups of six animals per group: (1) PBS (20 μL), (2) 660 nm laser alone, (3) 808 nm laser alone, (4) free Ce6 (5 mg/kg), (5) Ir-Me (5 mg/kg) and (6) Ir-Es (5 mg/kg). The mice were treated via intratumoral injection. For the irradiated groups, tumor tissues were irradiated with a laser beam (0.3mW/cm<sup>2</sup>) (660 nm laser beam for Ce6 group, 808 nm laser beam for Ir-Me and Ir-Es group) for 20 min at 2h post-injection. Mice of each group were treated with above formulations every four days for three times. After administration, the tumor size was measured with caliper and body weight was recorded every the other day for 21 days. Three weeks later, all the mice were sacrificed. The major organs and tumors were excised and weighed. The tumor volume was calculated as the following equation:  $V = (d^2 \times l) / 2$ , where  $d$  and  $l$  were the width and length of the tumor, respectively. The tumor growth inhibition (TGI) was calculated using the equation of  $TGI = W_0 / W_t \times 100\%$ , where  $W_0$  and  $W_t$  represented the tumor weight of PBS group and treated group, respectively.

### **Image processing and analysis**

Micrographs were processing and analyzed by ZEISS Imaging Browser and ImageJ 1.48v (32-bit). Quantification of the fluorescence intensity was achieve via Analyze >> Tools >> ROI manager in ImageJ from three parallel experiments. Quantification of single cell intensity profile was achieve via Analyze >> Plot Profile by selecting one cell in ImageJ. Quantification

of colocalization efficiency was achieved via an external plugin via Plugins >> Colocalization Finder. For more details, please refer to online sources: <https://imagej.nih.gov/ij/>.



**Scheme S1.** The synthetic routes for Ir complexes.

## Synthesis

### Synthesis of complexes Ir0

Complex Ir0 was synthesized according to the literature reported before [5].

### Synthesis of complex Ir-Es

Chloro-bridged dimer Ir complex Ir0 0.21g (0.19 mmol), and ethyl 4-(2,6-di(pyridine -2-yl)pyridin-4-yl)benzoate 0.15g (0.38 mmol) were added to 250 mL three neck flask. Then the mixtures were dissolved in 50 mL CH<sub>2</sub>Cl<sub>2</sub>:Methanol = 1:1 (v/v). The solution was heated to 60 °C under nitrogen atmosphere for 24 h. When the reaction finished, the reaction was cooled to room temperature. The mixtures were continuously stirred for 4 h after NH<sub>4</sub>PF<sub>6</sub> 0.31 g (1.92 mmol) was added. A bright orange solid was obtained by column chromatography on alumina using dichloromethane/methanol = 100/1 (v/v) as eluent. **Ir-Es:** 0.27g. Yield: 72%. Anal. Calcd. for C<sub>46</sub>H<sub>35</sub>N<sub>5</sub>O<sub>2</sub>IrPF<sub>6</sub>: C, 53.80; H, 3.44; N, 6.82. Found: C, 53.70; H, 3.48; N, 6.79. <sup>1</sup>H NMR (400 MHz, Acetonitrile-*d*<sub>3</sub>, δ): 8.84 (d, *J* = 1.6 Hz, 2H), 8.77 (d, *J* = 8.1 Hz, 1H), 8.20 (t, *J* = 6.4 Hz, 4H), 8.03 (t, *J* = 8.0 Hz, 3H), 7.96 (d, *J* = 8.4 Hz, 1H), 7.91 (d, *J* = 8.4 Hz, 1H), 7.87 (m, 1H), 7.82 (d, *J* = 6.4 Hz, 1H), 7.79, (d, *J* = 1.6 Hz, 1H), 7.71 (d, *J* = 7.6 Hz, 1H), 7.59 (d, *J* = 6 Hz, 1H), 7.47 (t, *J* = 6.6 Hz, 1H), 7.40 (d, *J* = 7.6 Hz, 1H), 7.2 (m, 2H), 6.97 (m, 3H), 6.77 (m, 2H), 6.62 (t, *J* = 7.5 Hz, 1H), 6.34 (t, *J* = 7.4 Hz, 1H), 5.91 (d, *J* = 7.6 Hz, 1H), 5.48 (d, *J* = 7.6 Hz, 1H), 4.40 (q, *J* = 7.1 Hz, 2H, CH<sub>2</sub>), 1.41 (t, *J* = 7.1 Hz, 3H, CH<sub>3</sub>). <sup>13</sup>C NMR (100 MHz,

Acetonitrile- $d_3$ ,  $\delta$ ) 167.78, 166.11, 165.24, 163.09, 157.60, 149.72, 148.19, 147.99, 138.84, 138.08, 137.98, 135.72, 131.85, 130.12, 129.84, 129.76, 129.22, 127.61, 127.54, 126.09, 125.36, 124.34, 123.78, 123.50, 122.67, 122.60, 122.32, 121.63, 120.25, 119.22, 119.12, 60.95, 13.23. MS (ESI)  $m/z$ :  $[M]^+$  Calculated for  $C_{46}H_{35}N_5O_2Ir$ , 882.24. Found 882.24.

### Synthesis of complex Ir-Me

Complex **Ir-Me** was synthesized in a similar manner to **Ir-Es** with using 2-(6-(pyridin-2-yl)-4-p-tolylpyridin-2-yl)pyridine 0.13g (0.38 mmol). A bright orange red solid was obtained. **Ir-Me**: 0.26g. Yield: 68 %. Anal. Calcd. for  $C_{44}H_{33}N_5IrPF_6$ : C, 54.54; H, 3.43; N, 7.23. Found: C, 54.47; H, 3.55; N, 7.16.  $^1H$  NMR (400 MHz, Acetonitrile- $d_3$ ,  $\delta$ ): 8.85 (s, 1H), 8.77 (dd,  $J = 13.9, 4.9$  Hz, 2H), 8.18 (t,  $J = 7.2$  Hz, 2H), 8.02 (d,  $J = 8.1$  Hz, 1H), 7.96 (d,  $J = 8.1$  Hz, 1H), 7.85 (m, 5H), 7.72 (dd,  $J = 12.4, 4.7$  Hz, 2H), 7.60 (d,  $J = 5.7$  Hz, 1H), 7.43 (m, 4H), 7.19 (dt,  $J = 7.7, 6.8$  Hz, 2H), 6.98 (dt,  $J = 13.1, 6.8$  Hz, 3H), 6.76 (m, 2H), 6.61 (t,  $J = 7.5$  Hz, 1H), 6.33 (t,  $J = 7.4$  Hz, 1H), 5.92 (d,  $J = 7.6$  Hz, 1H), 5.48 (d,  $J = 7.6$  Hz, 1H), 2.45 (s, 3H,  $CH_3$ ).  $^{13}C$  NMR (100 MHz, Acetonitrile- $d_3$ ,  $\delta$ ) 167.80, 166.15, 162.90, 157.33, 156.80, 155.75, 151.94, 150.57, 149.87, 149.64, 148.17, 147.92, 146.79, 143.20, 142.50, 141.32, 138.76, 138.04, 137.93, 135.67, 131.99, 131.83, 130.15, 129.81, 129.76, 129.18, 127.38, 127.18, 125.32, 125.23, 124.32, 123.68, 123.49, 122.64, 122.57, 122.28, 122.25, 120.97, 120.20, 119.18, 119.09. MS (ESI)  $m/z$ :  $[M]^+$  Calculated for  $C_{44}H_{33}N_5Ir$ , 824.24. Found 824.24.

### Synthesis of complex Ir-Pn

Complex **Ir-Pn** was synthesized in a similar manner to **Ir-Es** with using N,N-diethyl-4-(2,6-di(pyridin-2-yl)pyridin-4-yl)benzenamine 0.15g (0.38 mmol). A bright orange red solid was achieved. **Ir-Pn**: 0.27g. Yield: 65 %. Anal. Calcd. for  $C_{47}H_{40}N_6IrPF_6$ : C, 55.02; H, 3.93; N, 8.19. Found: C, 54.97; H, 3.96; N, 8.17.  $^1H$  NMR (400 MHz, Acetonitrile- $d_3$ ,  $\delta$ ): 8.88 (s, 1H), 8.72 (d,  $J = 8.2$  Hz, 1H), 8.68 (d,  $J = 1.6$  Hz, 1H), 8.17 (t,  $J = 7.6$  Hz, 2H), 8.01 (d,  $J = 8.0$  Hz, 1H), 7.96 (d,  $J = 8.1$  Hz, 1H), 7.86 (m, 4H), 7.79 (d,  $J = 5.3$  Hz, 1H), 7.70 (d,  $J = 7.7$  Hz, 1H), 7.63 (d,  $J = 1.7$  Hz, 1H), 7.60 (d,  $J = 5.7$  Hz, 1H), 7.42 (dd,  $J = 15.4, 7.5$  Hz, 2H), 7.21 (t,  $J = 6.6$  Hz, 1H), 7.15 (t,  $J = 7.7$  Hz, 1H), 6.96 (ddd,  $J = 12.0, 11.2, 6.0$  Hz, 3H), 6.84 (d,  $J = 9.0$  Hz, 2H), 6.77 (t,  $J = 7.5$  Hz, 1H), 6.69 (d,  $J = 7.4$  Hz, 1H), 6.60 (t,  $J = 7.5$  Hz, 1H), 6.32 (t,  $J = 7.4$  Hz, 1H), 5.92 (d,  $J = 7.7$  Hz, 1H), 5.47 (d,  $J = 7.6$  Hz, 1H), 3.48 (q,  $J = 6.8$  Hz, 4H,  $CH_2$ ), 1.19 (t,  $J = 6.8$  Hz, 6H,  $CH_3$ ).  $^{13}C$  NMR (100 MHz, Acetonitrile- $d_3$ ,  $\delta$ ) 167.86, 166.26, 162.53,

157.22, 156.90, 156.17, 151.95, 150.18, 150.09, 149.77, 149.52, 148.17, 147.85, 147.25, 143.29, 142.50, 138.62, 137.97, 137.84, 135.61, 131.81, 130.23, 129.78, 129.15, 128.47, 127.11, 124.97, 124.30, 123.51, 123.48, 122.97, 122.59, 122.51, 122.20, 120.11, 119.68, 119.13, 119.03, 118.92, 111.38, 43.82, 11.51. MS (ESI)  $m/z$ :  $[M]^+$  Calculated for  $C_{47}H_{40}N_6Ir$ , 881.29. Found 881.29.

### Synthesis of complex **Ir-Pc**

Complex **Ir-Pc** was synthesized in a similar manner to **Ir-Es** with using 2-(6-(pyridin-2-yl)-4-p-tolylpyridin-2-yl)pyridine 0.19g (0.38 mmol). A bright orange red solid was achieved. **Ir-Pc**: 0.28. Yield: 66 %. Anal. Calcd. for  $C_{51}H_{44}N_6O_2IrPF_6$ : C, 53.63; H, 3.88; N, 7.36. Found: C, 53.69; H, 3.92; N, 7.33.  $^1H$  NMR (400 MHz, Acetonitrile- $d_3$ ,  $\delta$ ): 8.83 (s, 1H), 8.73 (d,  $J = 8.8$  Hz, 2H), 8.17 (t,  $J = 7.2$  Hz, 2H), 8.01 (d,  $J = 8.1$  Hz, 1H), 7.96 (d,  $J = 8.2$  Hz, 1H), 7.85 (m, 5H), 7.69 (dd,  $J = 10.0, 4.6$  Hz, 2H), 7.60 (d,  $J = 5.6$  Hz, 1H), 7.42 (m, 2H), 7.16 (m, 2H), 6.96 (m, 3H), 6.78 (t,  $J = 8.9$  Hz, 3H), 6.70 (d,  $J = 7.7$  Hz, 1H), 6.61 (t,  $J = 7.2$  Hz, 1H), 6.32 (t,  $J = 7.4$  Hz, 1H), 5.92 (d,  $J = 7.5$  Hz, 1H), 5.48 (d,  $J = 7.5$  Hz, 1H), 4.21 (dd,  $J = 14.6, 7.5$  Hz, 8H,  $CH_2$ ), 1.28 (t,  $J = 7.2$  Hz, 6H,  $CH_3$ ).  $^{13}C$  NMR (100 MHz, Acetonitrile- $d_3$ ,  $\delta$ ) 169.69, 167.85, 166.23, 162.70, 157.05, 150.08, 149.58, 148.19, 147.91, 147.05, 143.26, 142.52, 138.69, 138.00, 137.88, 135.62, 131.82, 130.19, 129.80, 129.15, 128.37, 127.23, 125.06, 124.30, 123.93, 123.57, 123.50, 123.03, 122.63, 122.53, 122.24, 120.15, 119.76, 119.16, 119.05, 112.29, 60.69, 52.49, 13.24. MS (ESI)  $m/z$ :  $[M]^+$  Calculated for  $C_{51}H_{44}N_6O_2$ , 997.31. Found 997.31.

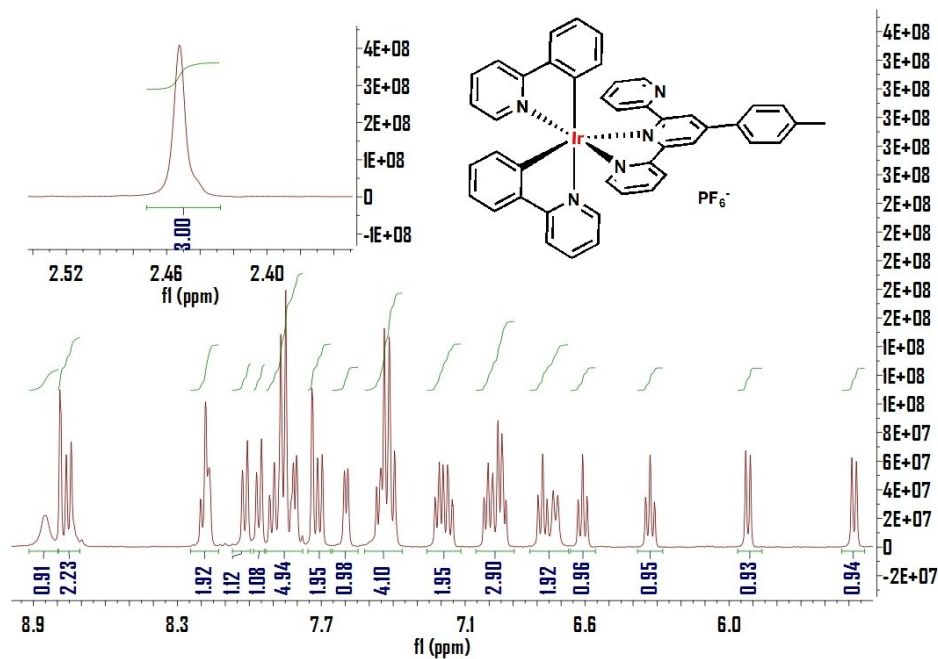
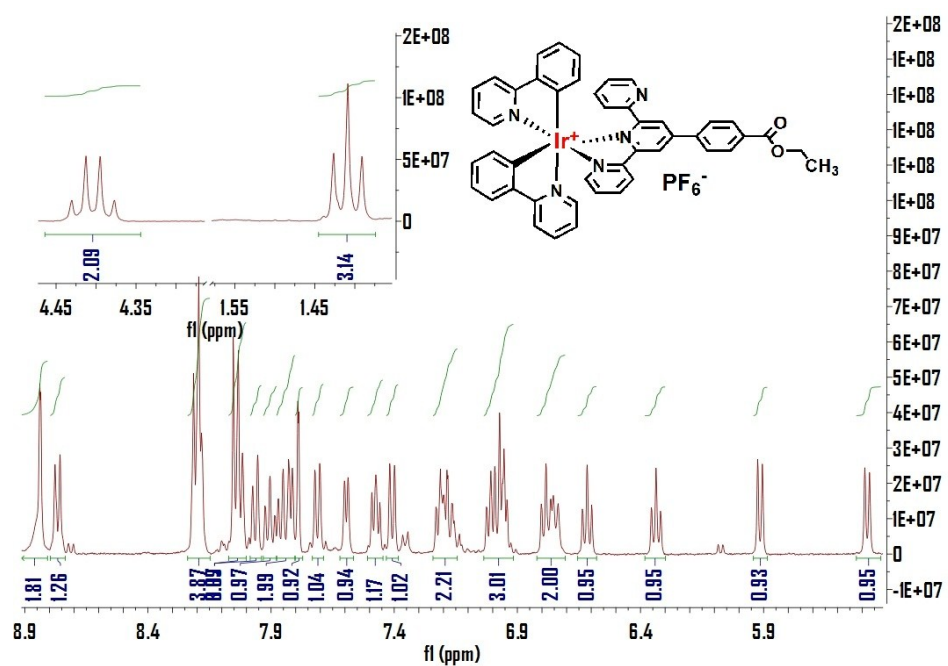
### Synthesis of complex **Ir-Cz**

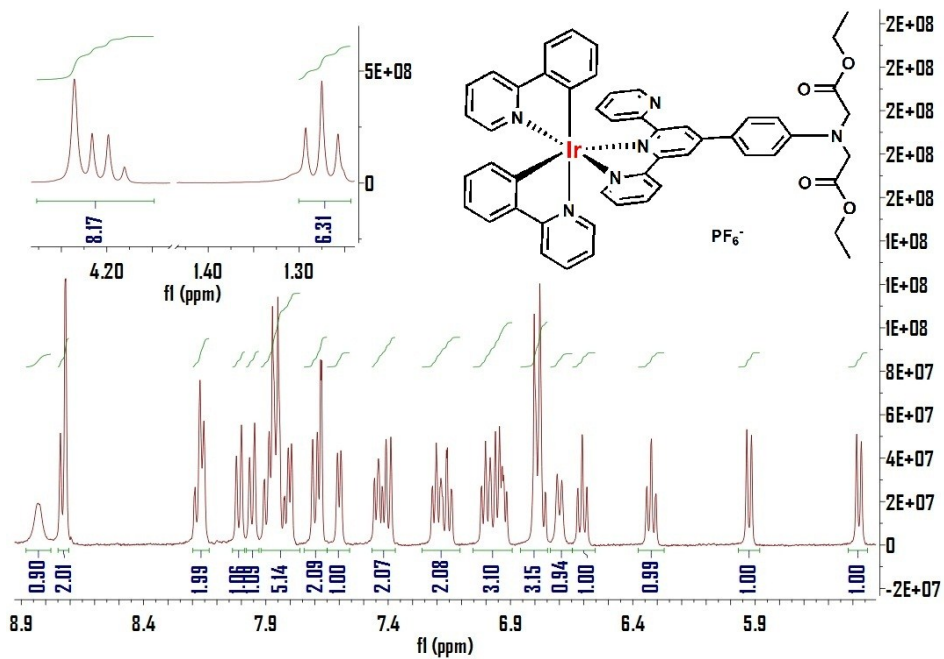
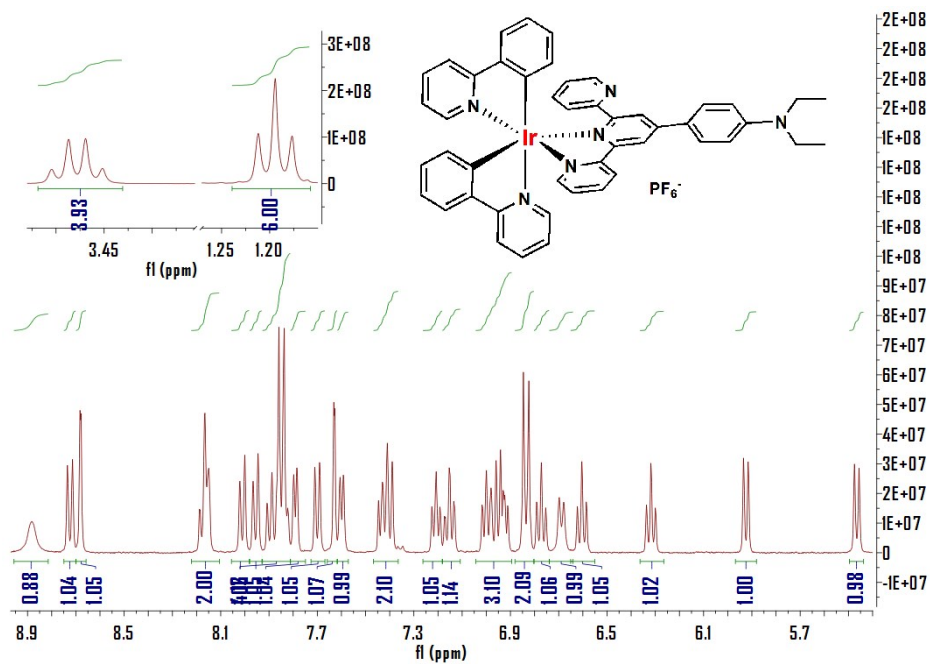
Complex **Ir-Cz** was synthesized in a similar manner to **Ir-Es** with using 2-(6-(pyridin-2-yl)-4-p-tolylpyridin-2-yl)pyridine 0.20g (0.38 mmol). A bright orange red solid was achieved. **Ir-Cz**: 0.26. Yield: 61 %. Anal. Calcd. for  $C_{54}H_{44}N_6O_2IrPF_6$ : C, 56.59; H, 3.87; N, 7.33. Found: C, 56.57; H, 3.91; N, 7.34.  $^1H$  NMR (400 MHz, Acetonitrile- $d_3$ ,  $\delta$ ): 8.99 (d,  $J = 1.9$  Hz, 1H), 8.95 (d,  $J = 8.2$  Hz, 1H), 8.86 (m, 2H), 8.28 (d,  $J = 7.7$  Hz, 1H), 8.18 (m, 2H), 8.07 (dd,  $J = 8.7, 1.8$  Hz, 1H), 7.98 (m, 3H), 7.86 (m, 4H), 7.69 (m, 2H), 7.61 (dd,  $J = 11.4, 6.3$  Hz, 2H), 7.54 (dd,  $J = 8.4$  Hz, 1H), 7.43 (m,  $J = 17.3, 8.3, 6.0$  Hz, 2H), 7.30 (t,  $J = 7.1$  Hz, 1H), 7.19 (m, 2H), 6.95 (m, 3H), 6.76 (m, 2H), 6.60 (t,  $J = 7.2$  Hz, 1H), 6.32 (td,  $J = 7.5, 1.2$  Hz, 1H), 5.91 (dd,  $J = 7.6, 0.7$  Hz, 1H), 5.47 (d,  $J = 7.1$  Hz, 1H), 4.56 (m, 2H,  $CH_2$ ), 3.88 (dd,  $J = 6.5, 4.2$  Hz, 2H,  $CH_2$ ), 3.47 (m, 2H,  $CH_2$ ), 3.34 (m, 2H,  $CH_2$ ), 3.15 (s, 3H,  $CH_3$ ).  $^{13}C$  NMR (100 MHz, Acetonitrile- $d_3$ ,  $\delta$ ) 168.68, 167.05, 163.58, 158.05, 157.88, 152.17, 150.90, 150.41, 149.04, 148.76, 147.95,

144.09, 142.88, 141.90, 139.61, 138.87, 138.76, 136.51, 132.68, 131.02, 130.66, 130.03, 128.11, 127.09, 126.23, 125.94, 125.70, 125.50, 125.17, 124.48, 124.35, 124.05, 123.50, 123.45, 123.21, 123.14, 123.06, 121.57, 121.16, 121.00, 120.76, 120.44, 120.03, 110.98, 110.58, 78.88, 78.55, 78.23, 72.08, 70.87, 69.65, 58.46, 43.86. MS (ESI)  $m/z$ :  $[M]^+$  Calculated for  $C_{54}H_{44}N_6O_2$ , 1001.32. Found 1001.32.

### Synthesis of complex Ir(bpy)

Complex Ir(bpy) was synthesized according to the literature reported before [6].





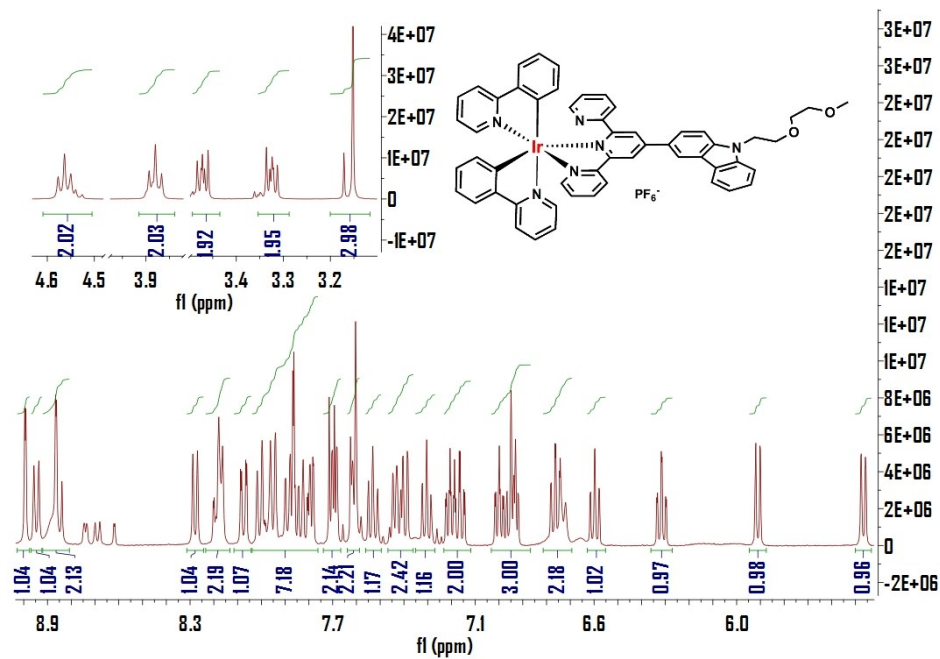


**Fig. S1.**  $^1\text{H}$  NMR spectra of the five Ir complexes (**Ir-Es**, **Ir-Me**, **Ir-Pn**, **Ir-Pc**, and **Ir-Cz**) in  $\text{CD}_3\text{CN}$

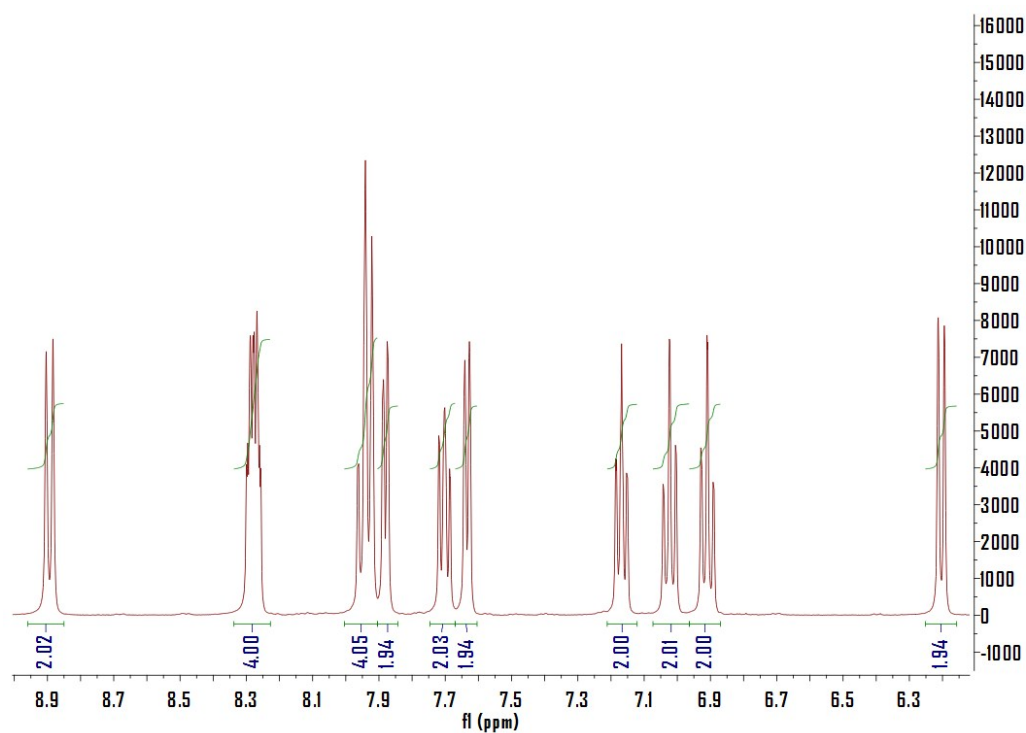
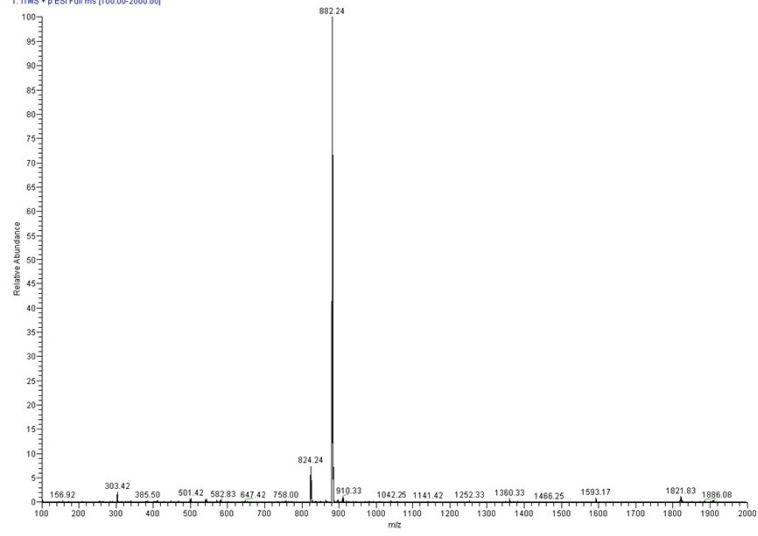
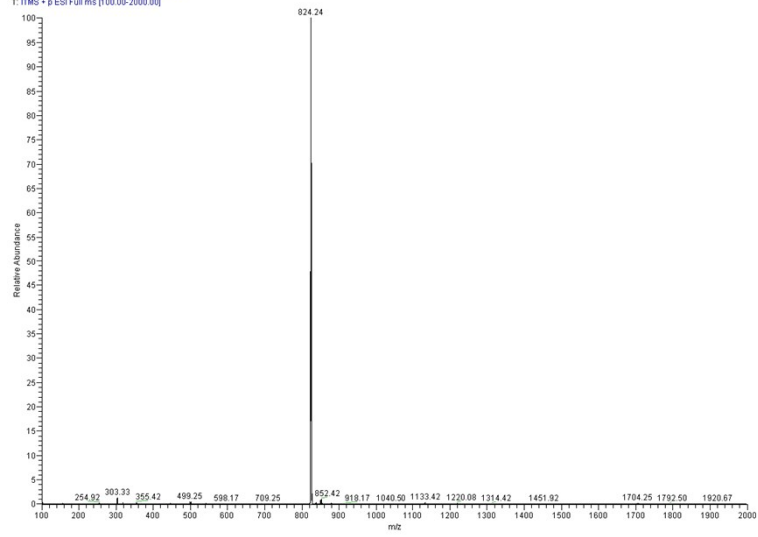


**Fig. S2.** The  $^1\text{H}$  NMR spectrum of Ir-(bpy).

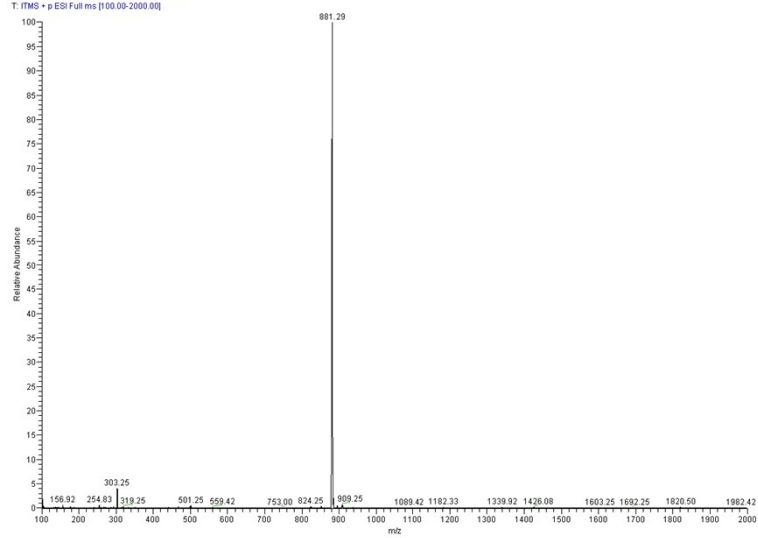
I3 #16-19 RT: 0.07-0.08 AV: 4 NL: 9.16E4  
T: ITMS - p ESI Full ms [100.00-2000.00]



I2 #15-25 RT: 0.07-0.11 AV: 11 NL: 1.21E5  
T: ITMS - p ESI Full ms [100.00-2000.00]



I10 #14-32 RT: 0.06-0.14 AV: 19 NL: 3.05E4  
T: ITMS - p ESI Full ms [100.00-2000.00]



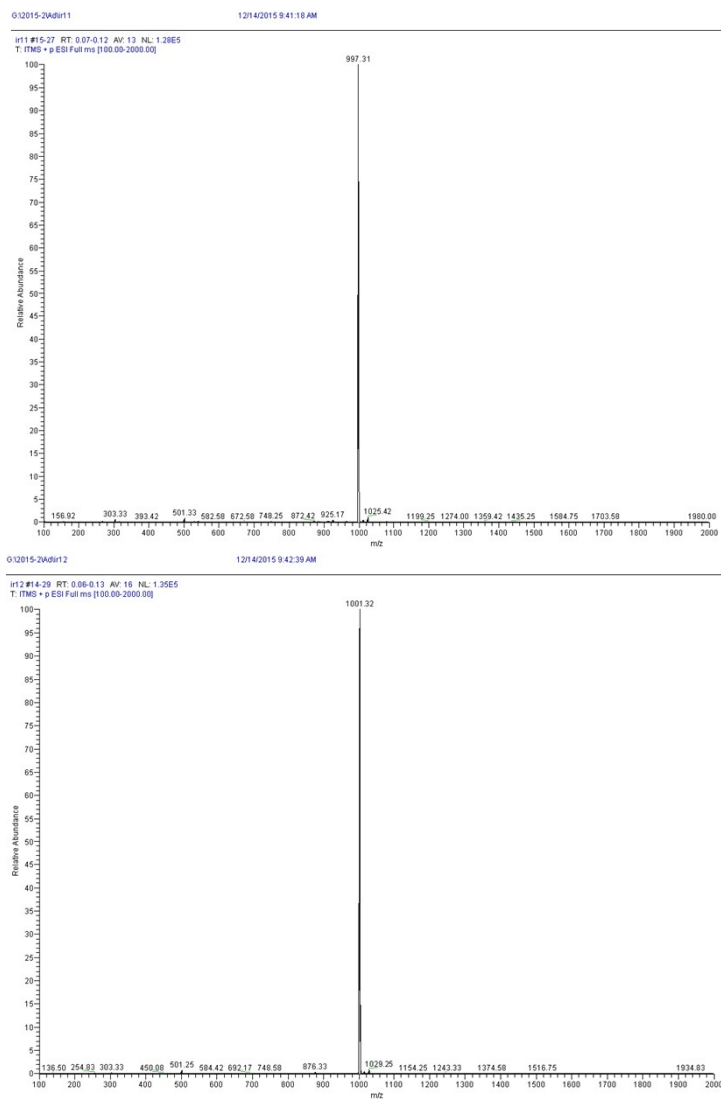


**Fig. S3.** ESI-MS spectra of the five Ir complexes (**Ir-Es**, **Ir-Me**, **Ir-Pn**, **Ir-Pc**, and **Ir-Cz**)

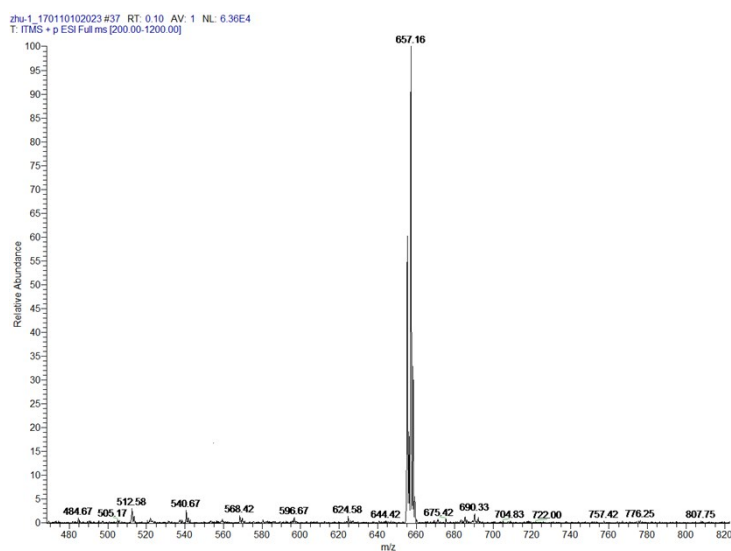


**Fig. S4.** The ESI-MS spectrum of Ir-(bpy).

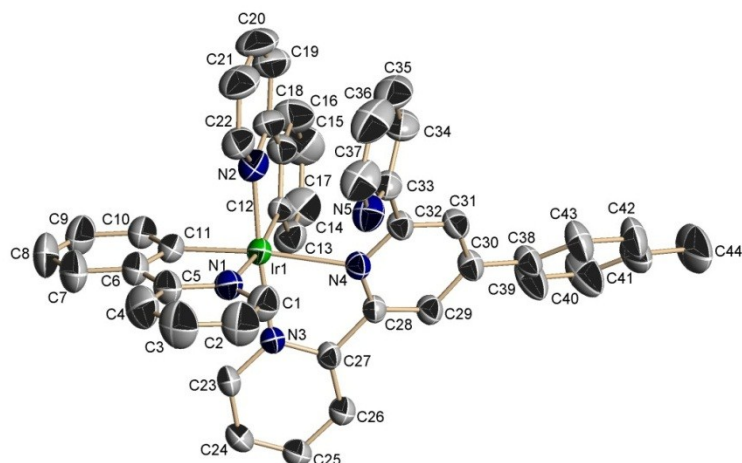


**Fig. S5.** The crystal structure of complexes **Ir-Me** (H atoms, solvent molecules, and anion have been omitted for clarity; thermal ellipsoids are drawn at 50 % probability)

**Table S1.** Crystal data collection and structure refinement for **Ir-Me**

Complex	Ir-Me
Empirical formula	C <sub>91</sub> H <sub>69</sub> N <sub>10</sub> P <sub>2</sub> F <sub>12</sub> Cl <sub>9</sub>
CCDC NO.	1509956
Formula weight	2295.95
Temperature	296(2) K
Wavelength	0.71073 Å
Space group	P <sub>1</sub>
Crystal system	Triclinic
<i>a</i> /Å	10.711(1)
<i>b</i> /Å	14.712(1)
<i>c</i> /Å	16.480(1)
$\alpha$ (°)	96.836(1)
$\beta$ (°)	94.980(1)
$\gamma$ (°)	109.659(1)
Volume Å <sup>3</sup>	2617 (2)
<i>Z</i>	1
Dc/Mg m <sup>-3</sup>	1.248
$\mu$ /mm <sup>-1</sup>	3.118
<i>F</i> (000)	1130
Final R indices	R <sub>1</sub> = 0.0365,
[I > 2 $\sigma$ (I)]	wR <sub>2</sub> = 0.1125
Goodness-of-fit on F <sup>2</sup>	1.067

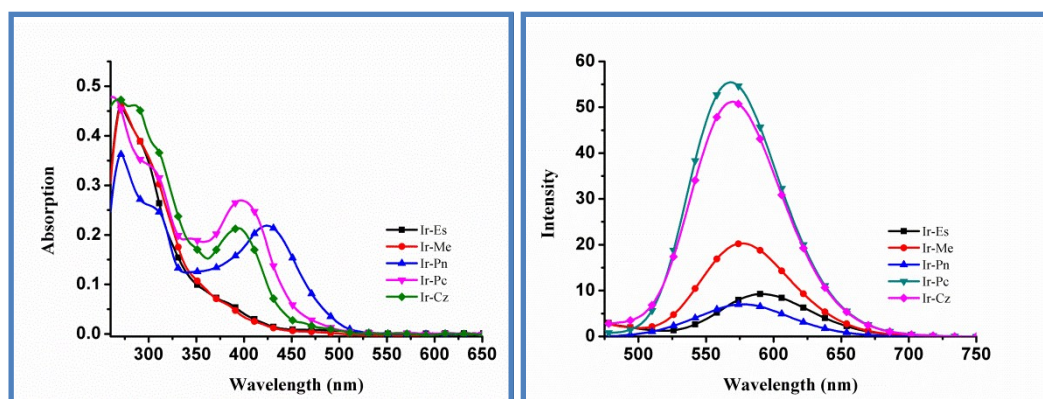


**Fig. S6.** The UV-vis absorption spectra (left) and luminescent spectra (right) of Ir complexes (**Ir-Es**, **Ir-Me**, **Ir-Pn**, **Ir-Pc**, and **Ir-Cz**) in dichloromethane ( $c = 1 \times 10^{-5}$  M).

**Table S2.** The photophysical properties of complexes **Ir-Me** and **Ir-Es** in dichloromethane

Complex	$\lambda_{\text{abs}}/\text{nm}(\log \epsilon)$	$\lambda_{\text{em}}^{\text{a}}$	$\Phi_{\text{em}}^{\text{b}}$	$\tau^{\text{c}}$ (ns)	Stokes Shift (nm)
<b>Ir-Es</b>	294 (4.62), 376 (3.83)	596	0.071	24, 50	220
<b>Ir-Me</b>	287 (4.66), 375 (3.97)	580	0.157	47, 78	205
<b>Ir-Pn</b>	270 (3.64), 304 (2.56), 424 (2.20)	580	0.010	6, 188	156
<b>Ir-Pc</b>	262 (4.78), 301 (3.42), 396 (2.70)	568	0.099	60, 101	172
<b>Ir-Cz</b>	268 (4.76), 307 (3.77), 392 (2.16)	570	0.135	43, 88	178

a. Peak position of fluorescence. b. Quantum yields determined by using  $[\text{Ru}(\text{bpy})_3]^{2+}$  as standard. c. The fitted fluorescence lifetime (ns)

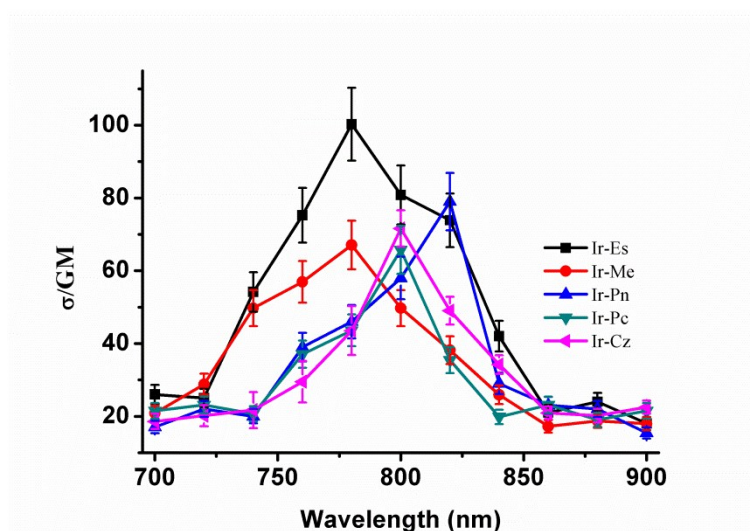


**Fig. S7.** Two-photon absorption cross sections of five Ir(III) complexes in dichloromethane with excited wavelength from 700 nm to 900 nm

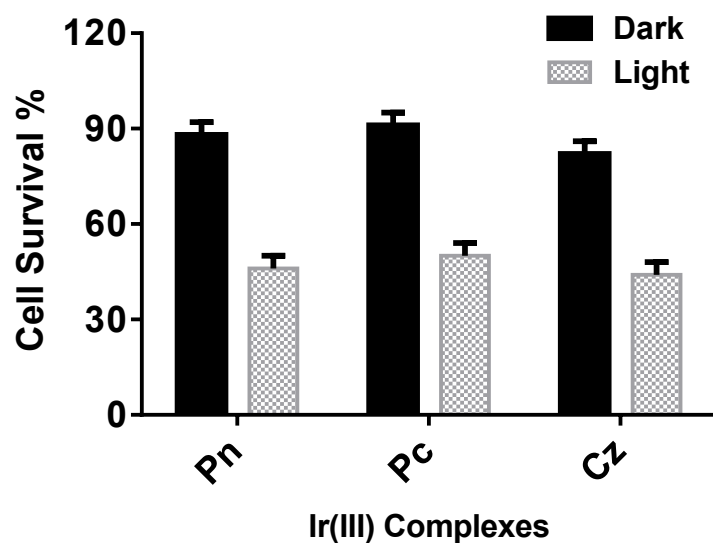


**Fig. S8.** HepG2 cells toxicity data under dark and UV light condition (interval=6 hours, 5 minutes/time, concentration 10  $\mu$ M) for **Ir-Pn**, **Ir-Pc**, and **Ir-Cz** obtained from the MTT assay after incubated for 24 h.

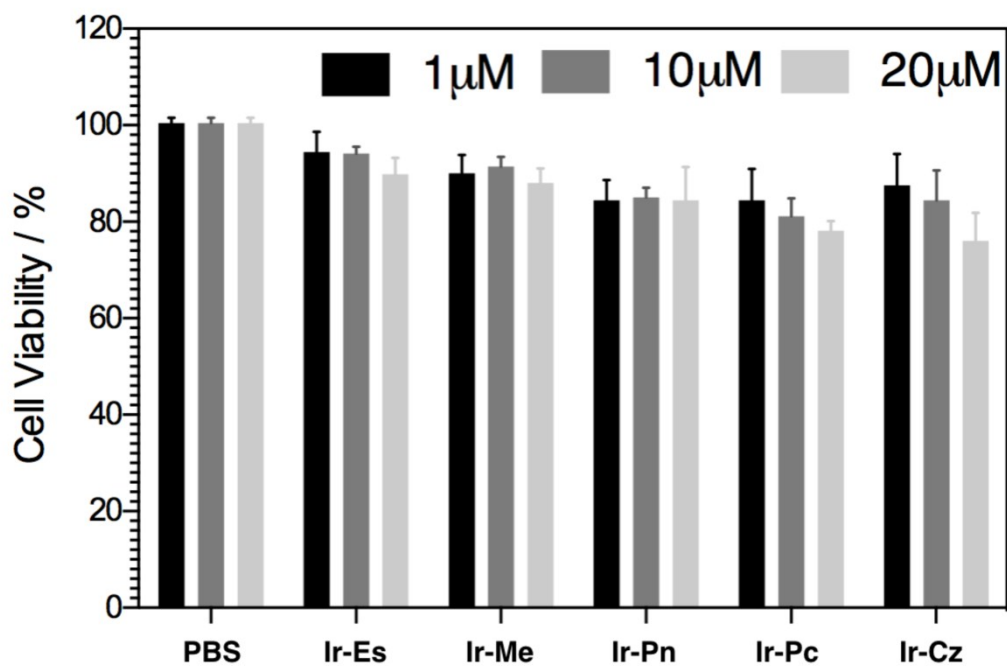


**Fig. S9.** Normal cells HELF toxicity data results of **Ir-Es**, **Ir-Me**, **Ir-Pn**, **Ir-Pc** and **Ir-Cz** ( $c = 1, 10, 20 \mu$ M) obtained from the MTT assays after incubation for 24 h.

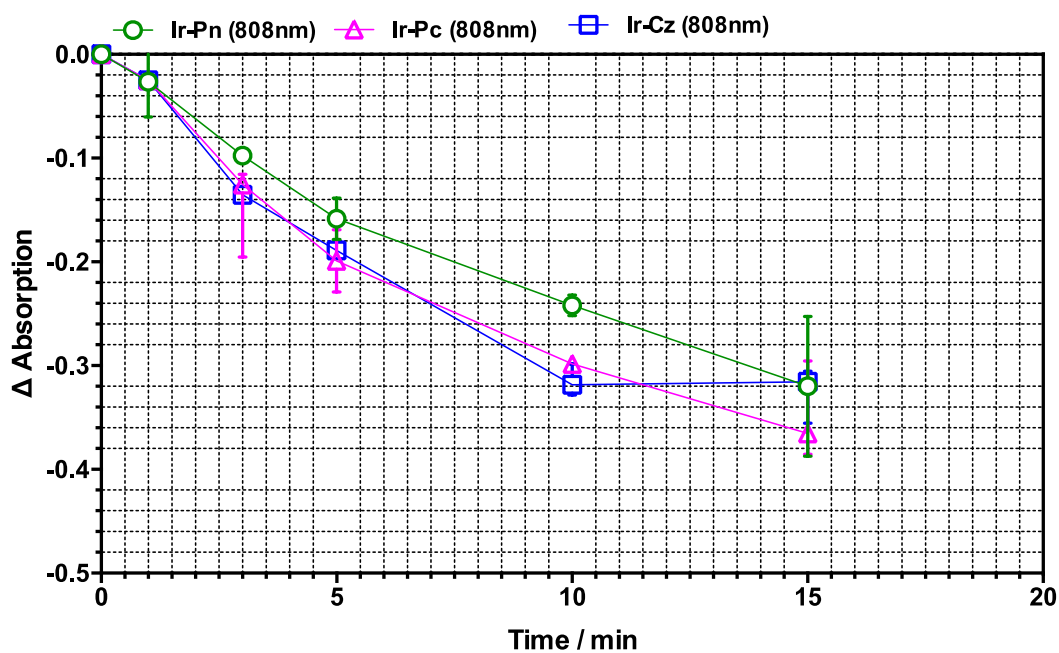


**Fig. S10.** The decrease of absorption of ADPA (100  $\mu$ M in PBS mixed with 5  $\mu$ M **Ir-Pn**, **Ir-Pc** and **Ir-Cz**, respectively) with laser exposure for 1, 3, 5, 10, 15 min.

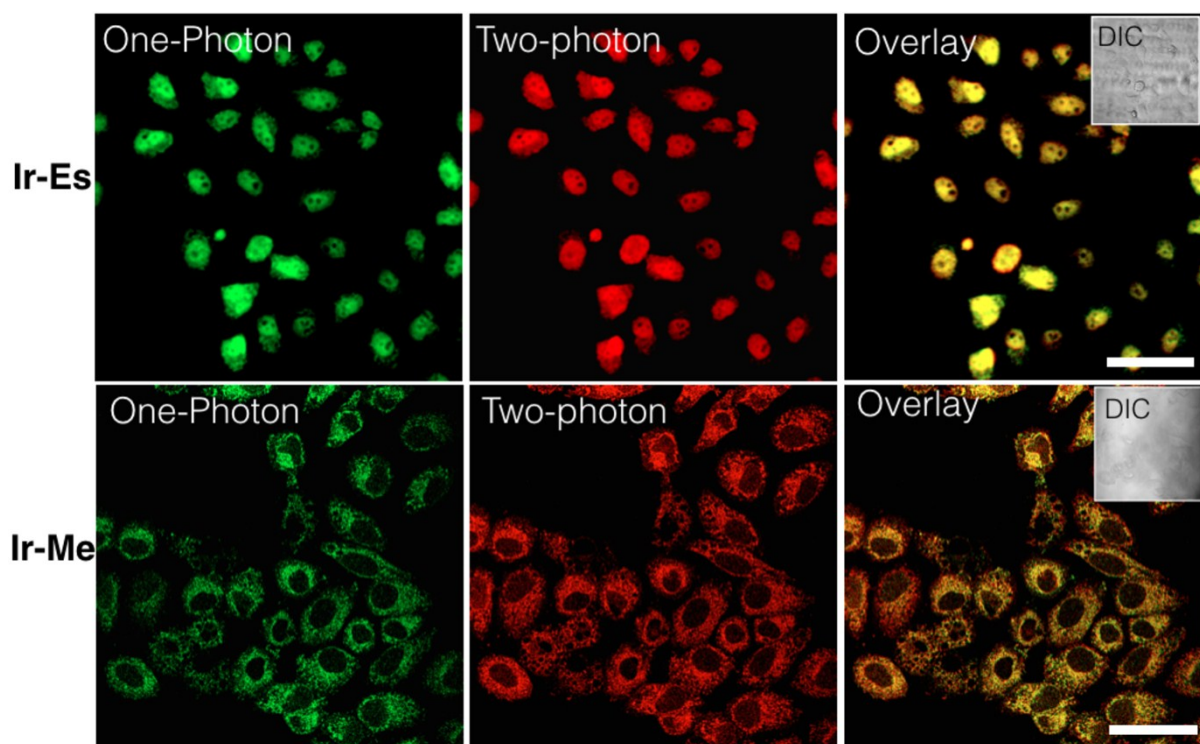


**Fig. S11.** Confocal micrographs (one-photon and two-photon) of HepG2 cells incubated with **Ir-Es** and **Ir-Me** complex (5  $\mu$ M). The scale bar represents 20  $\mu$ m.

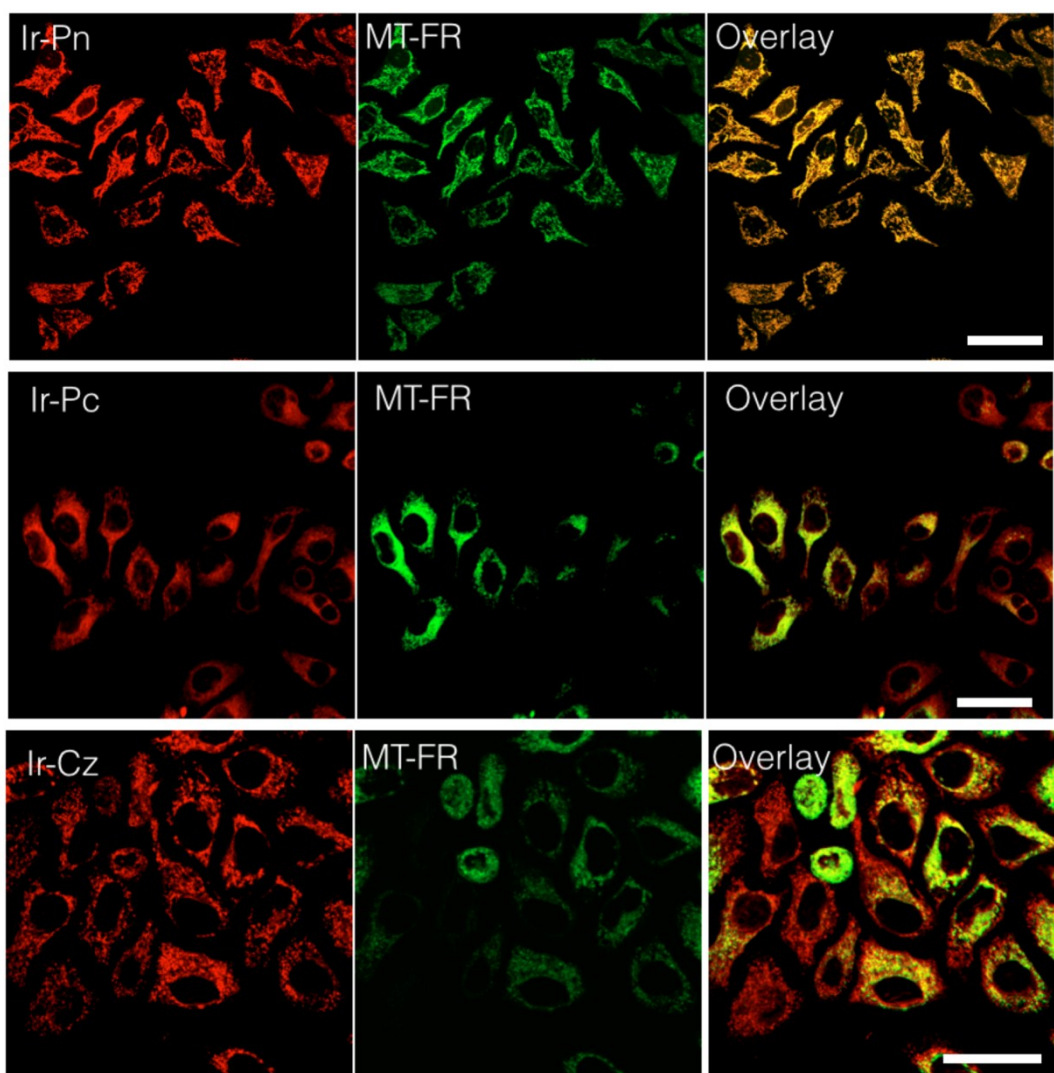


**Fig. S12.** Confocal micrographs (one-photon and two-photon) of HepG2 cells incubated with **Ir-Pn**, **Ir-Pc**, and **Ir-Cz** (5  $\mu\text{M}$ ). The scale bar represents 20  $\mu\text{m}$ .

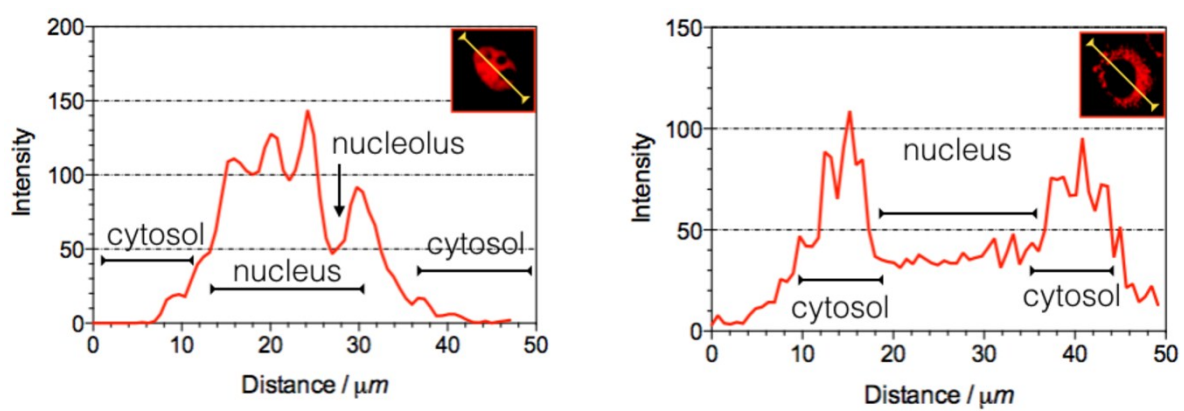


**Fig. S13.** Single cell intensity profile of HepG2 cells uptake **Ir-Es** and **Ir-Me** complex.

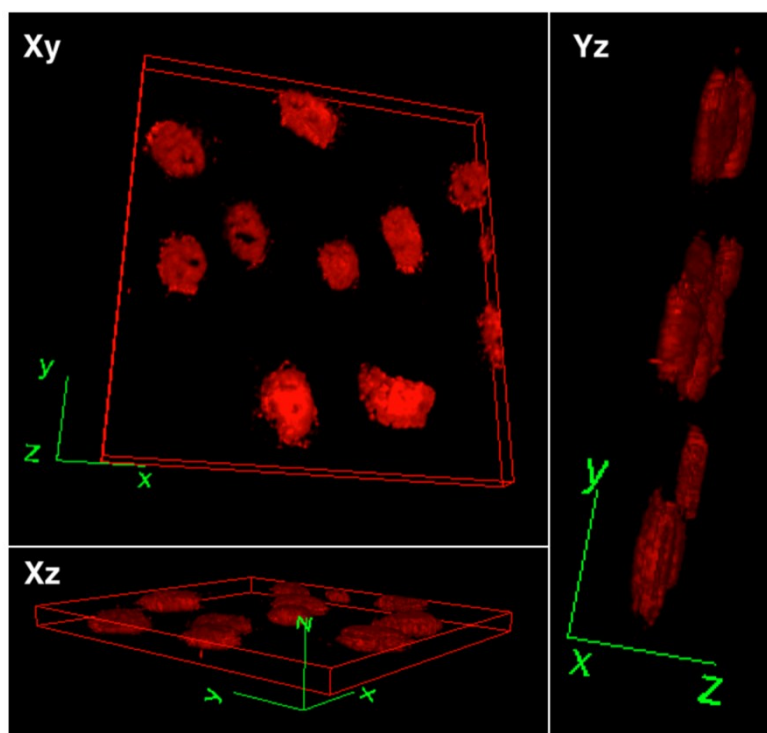


**Fig. S14.** 3D fluorescence imaging photograph of live HepG2 cells incubated with 5  $\mu\text{M}$  Ir-Es for 30 min at 37  $^{\circ}\text{C}$

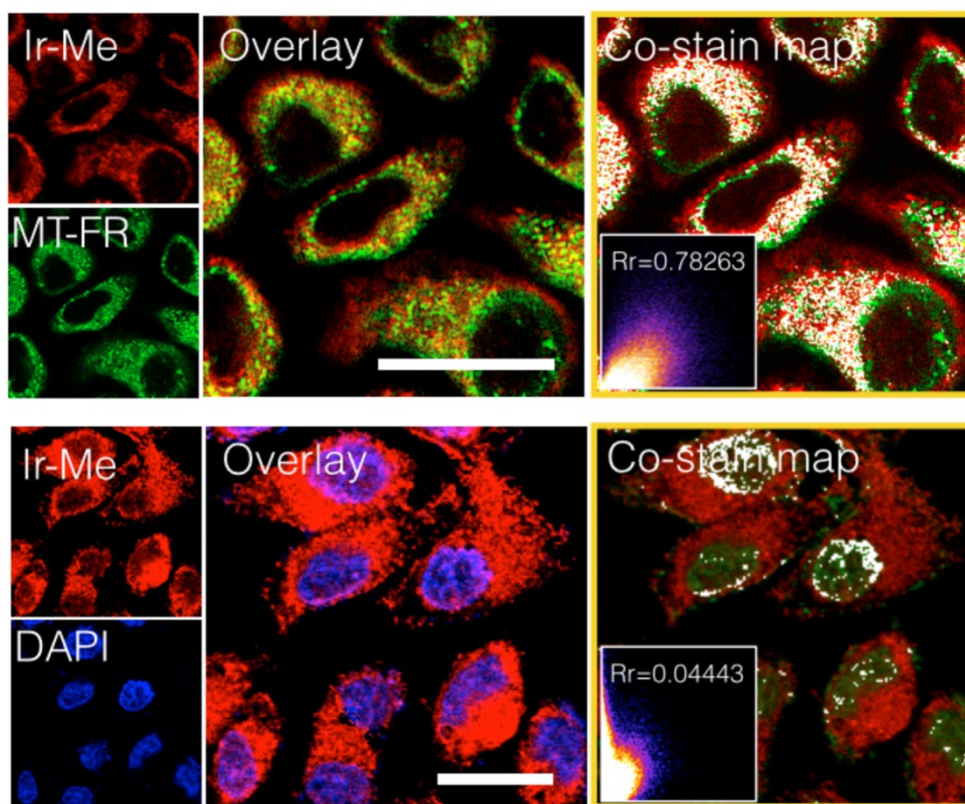


**Fig. S15.** Co-localization studies of Ir-Me with Mito-FR and DAPI. Insert: colocalization profile and Rr number showed the overlap coefficient. Scale bar = 10  $\mu\text{m}$ .

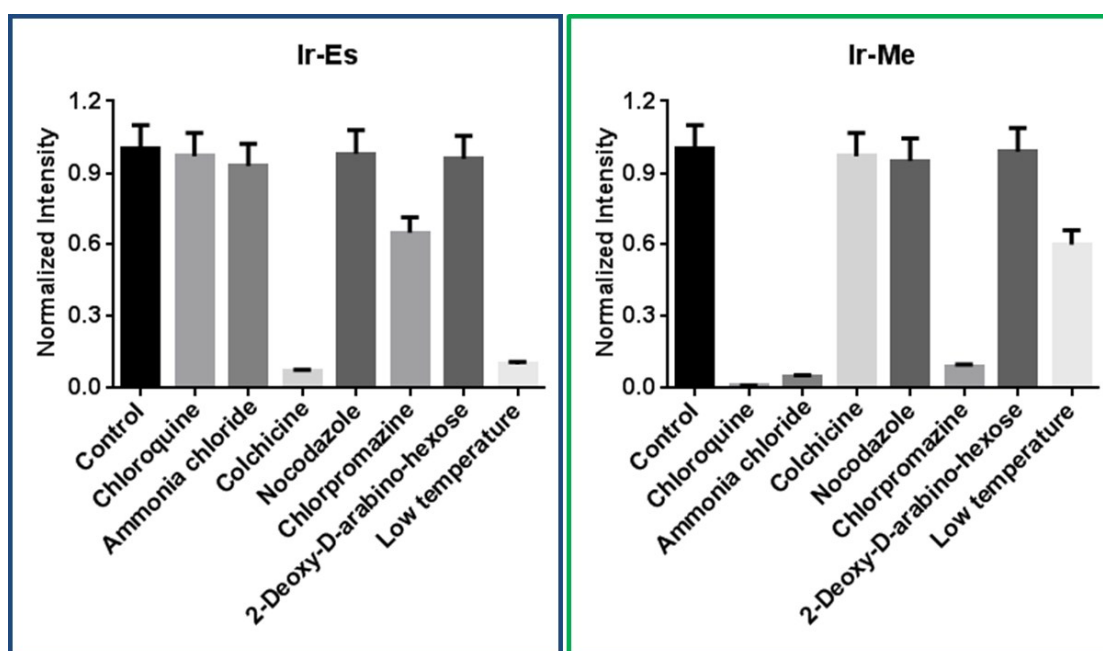


**Fig. S16.** The cell uptake inhibited experiment of **Ir-Me** and **Ir-Es** with six typical inhibitors.

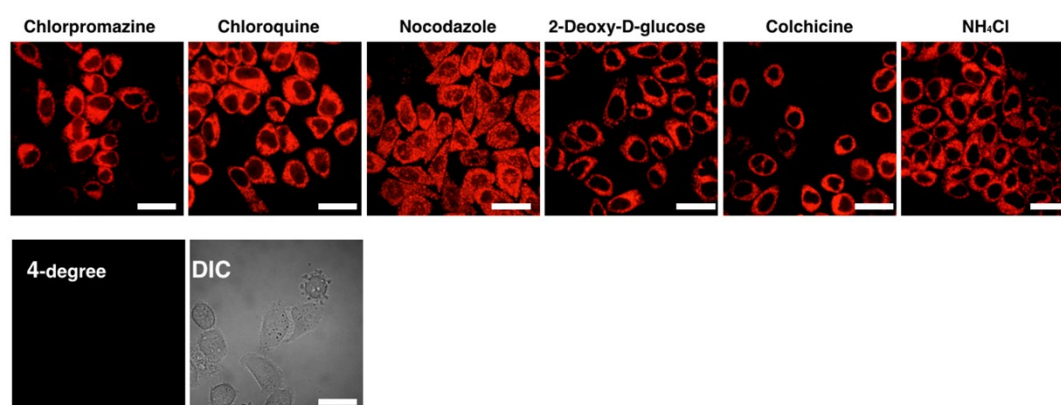


**Fig. S17.** The cell entry inhibitors experiment of **Ir-Pc** treat with six typical inhibitors and low temperature experiment. Scale bar=5  $\mu\text{m}$ .

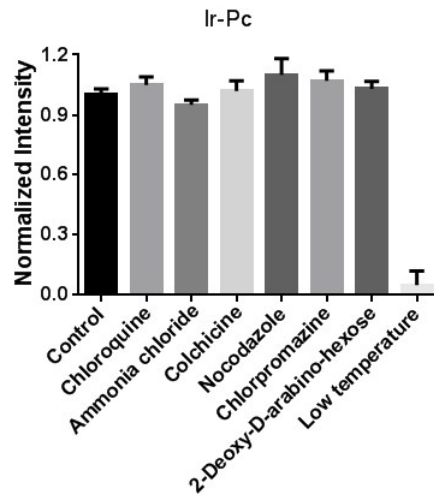


**Fig. S18.** The normalized cell uptake intensity from Fig. S17.

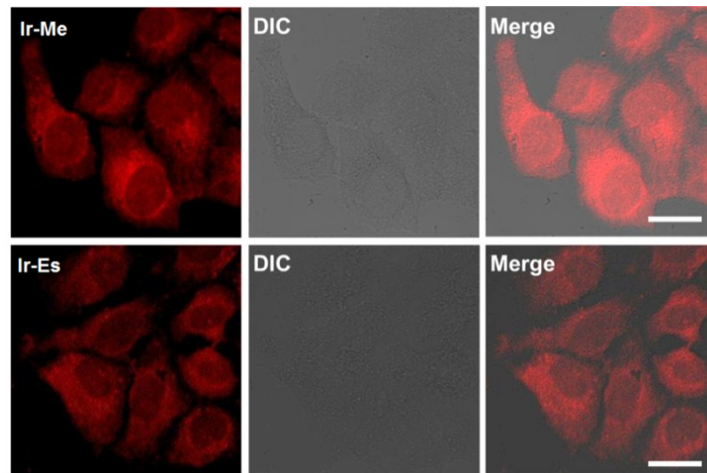


**Fig. S19.** Confocal microscopy imaging of fixed HepG2 cell incubated with **Ir-Me** and **Ir-Es** for 30 min. Scale bar = 10  $\mu\text{m}$ .

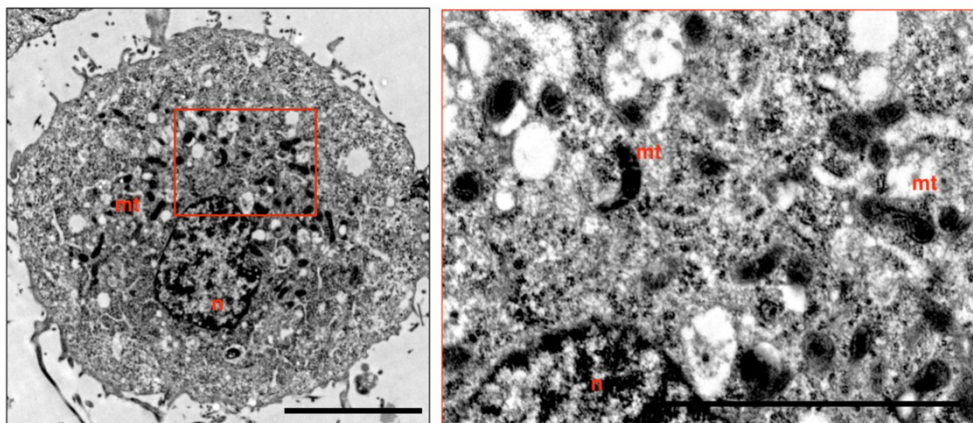


**Fig. S20.** TEM imaging of HepG2 cell incubated with **Ir-Me** without  $\text{OsO}_4$ . Scale bar = 5  $\mu\text{m}$ .

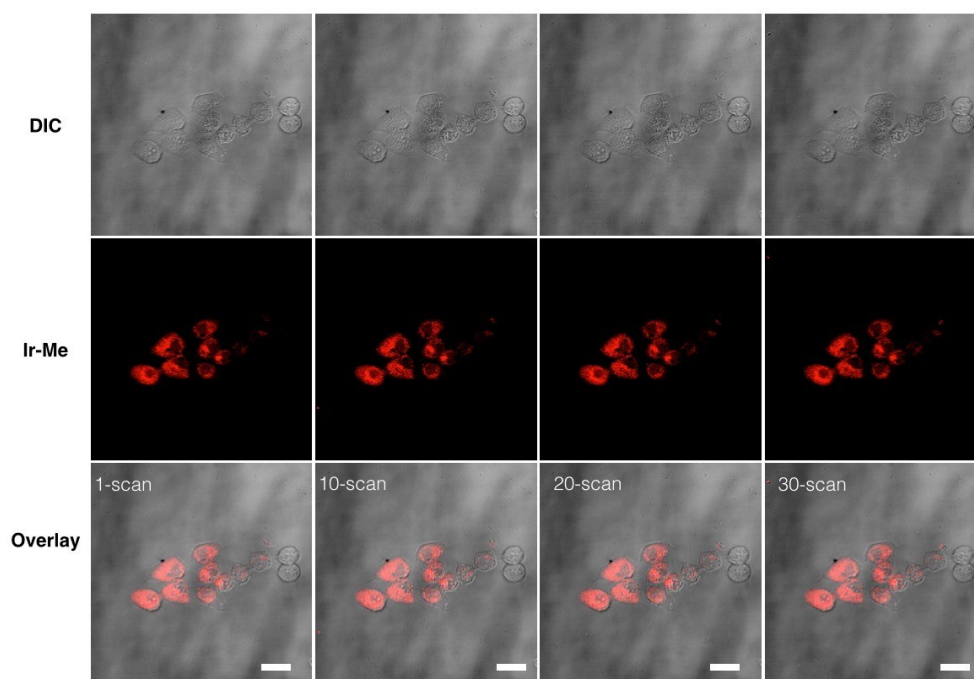


**Fig. S21.** Ir-Me PDT effect in HepG2 cells. Scale bar = 10  $\mu\text{m}$ .

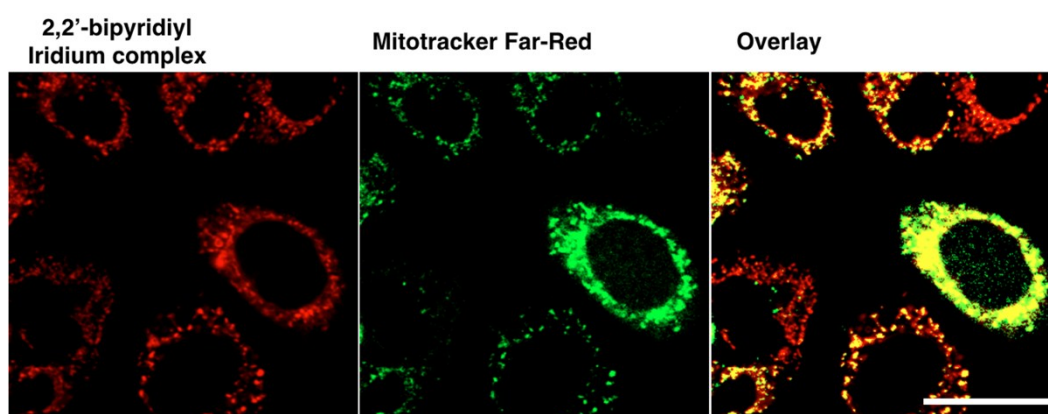


**Fig. S22.** The co-localization experiment using Ir-(bpy) complex and mitochondrial tracker Mitotracker Far-red. Scale bar= 5  $\mu\text{m}$ .

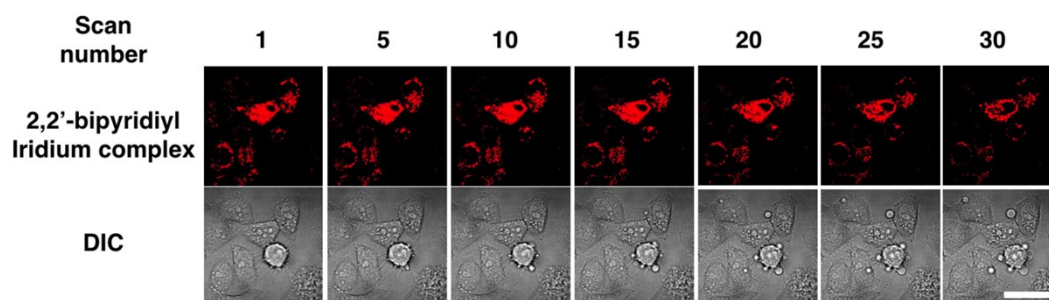


**Fig. S23.** The PDT experiment using Ir-(bpy) complex for continued 30-time scanning.

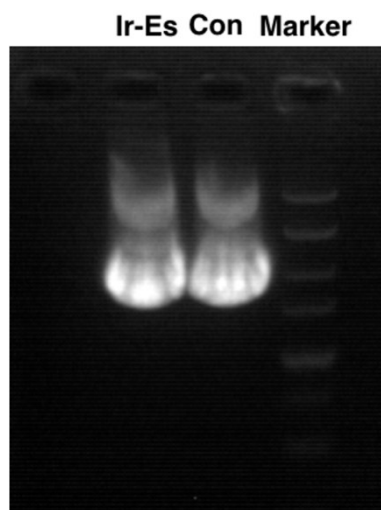


**Fig. S24.** DNA cleavage effect using Ir-Es complex under inhibition of  $^1\text{O}_2$ .

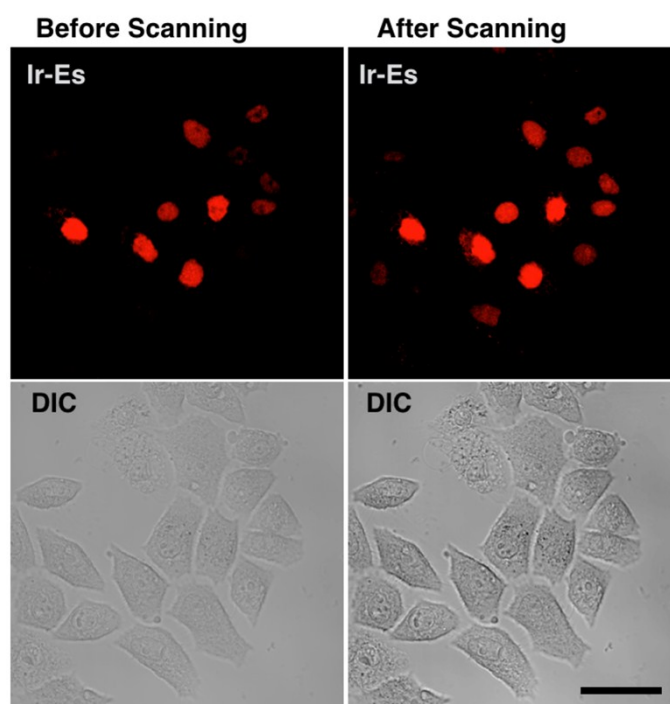


**Fig. S25.** PDT performance of Ir-Es complex under hypoxia condition; Scale bar=5 $\mu\text{m}$ .

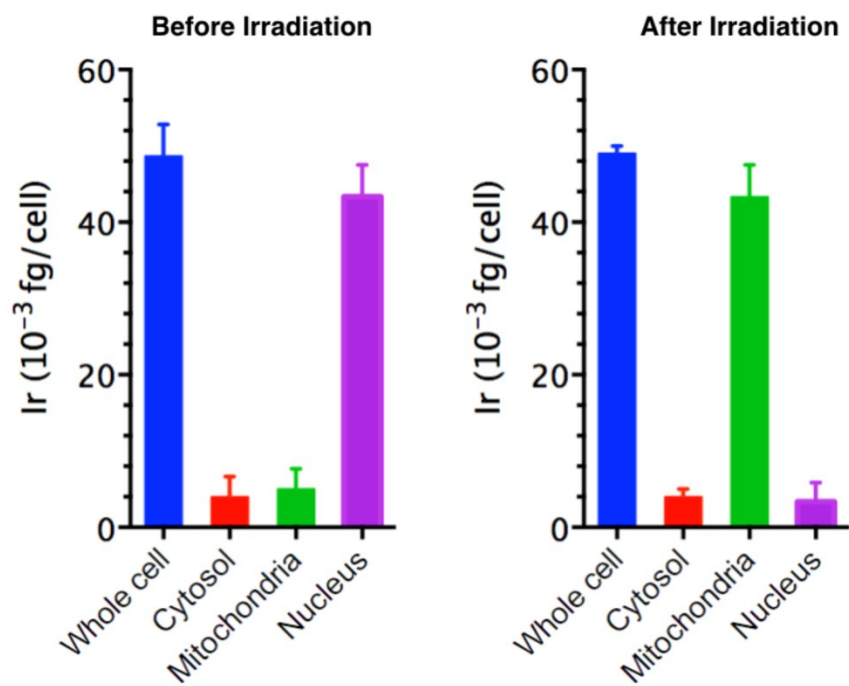


**Fig. S26.** ICP-MS quantifications of Iridium (**Ir-Es**) in different subcellular organelles before and after UV irradiation.

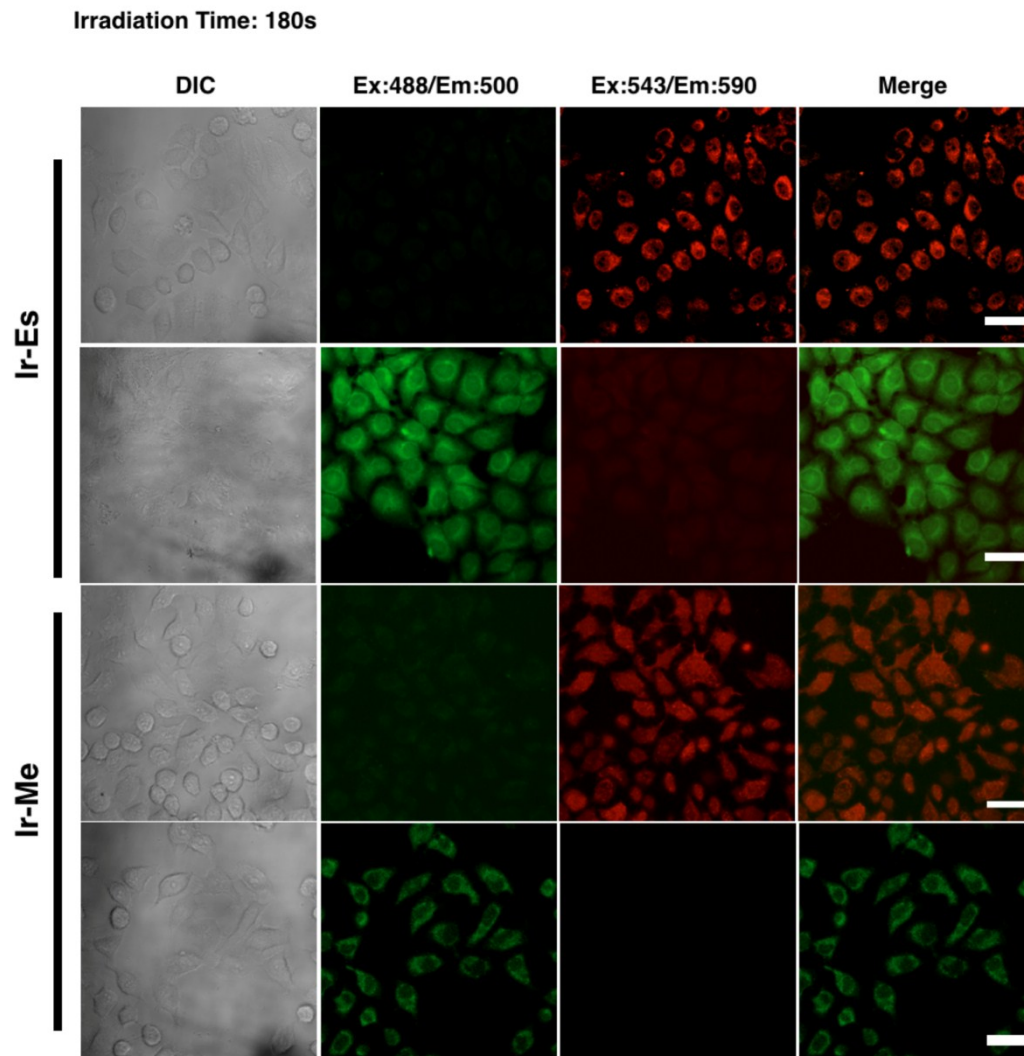


**Fig. S27.** Confocal fluorescence images of JC-1 stained HepG2 cells pre-treated with **Ir-Es** and **Ir-Me** under different irradiation time. Scale bar = 10  $\mu\text{m}$ .

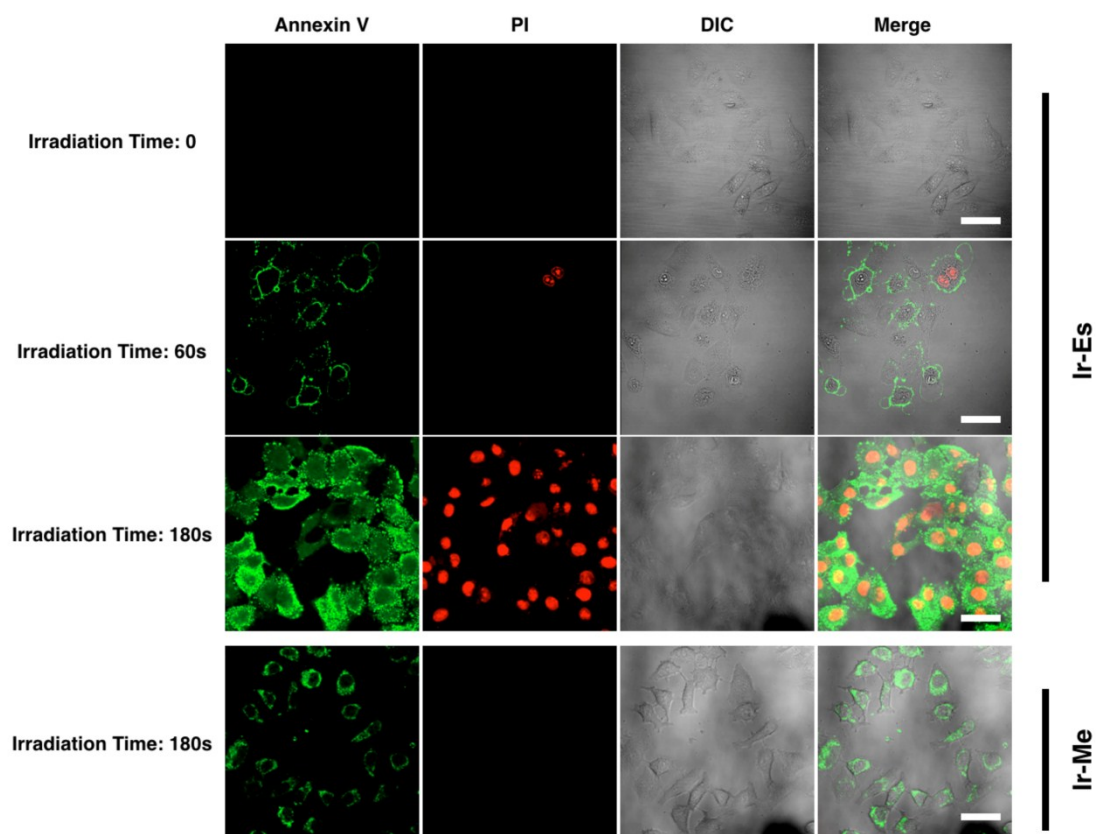


**Fig. S28.** Confocal fluorescence images of Annexin V-FITC/PI stained HepG2 cells pre-treated with **Ir-Es** and **Ir-Me** under different irradiation time. Scale bar = 10  $\mu\text{m}$ .

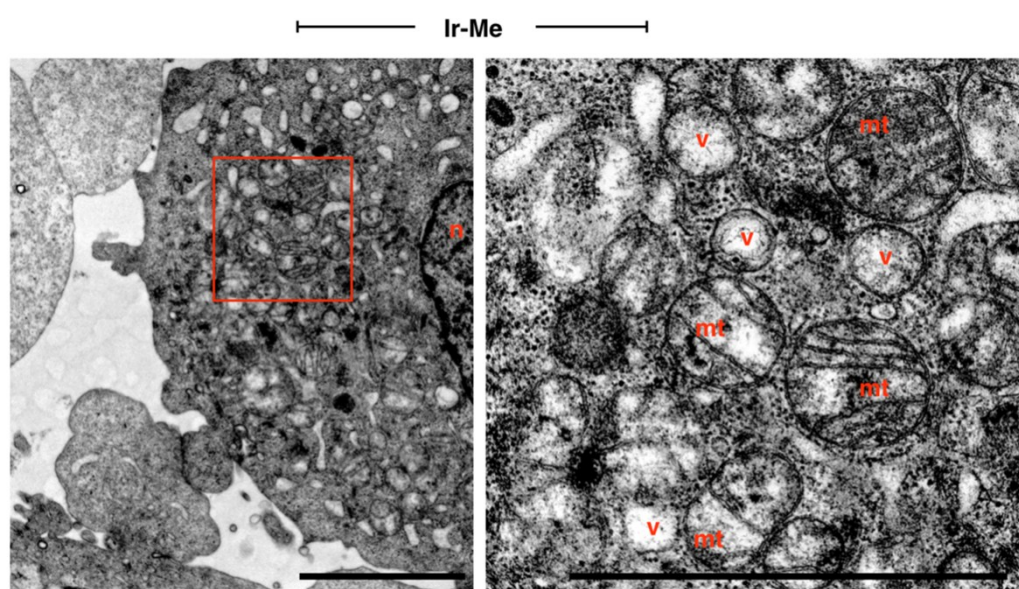


**Fig. S29.** TEM imaging of HepG2 cell incubated with **Ir-Me** with  $\text{OsO}_4$  and treated under UV light (illumination = 30 s, interval = 30 min). Scale bar = 5  $\mu\text{m}$ .

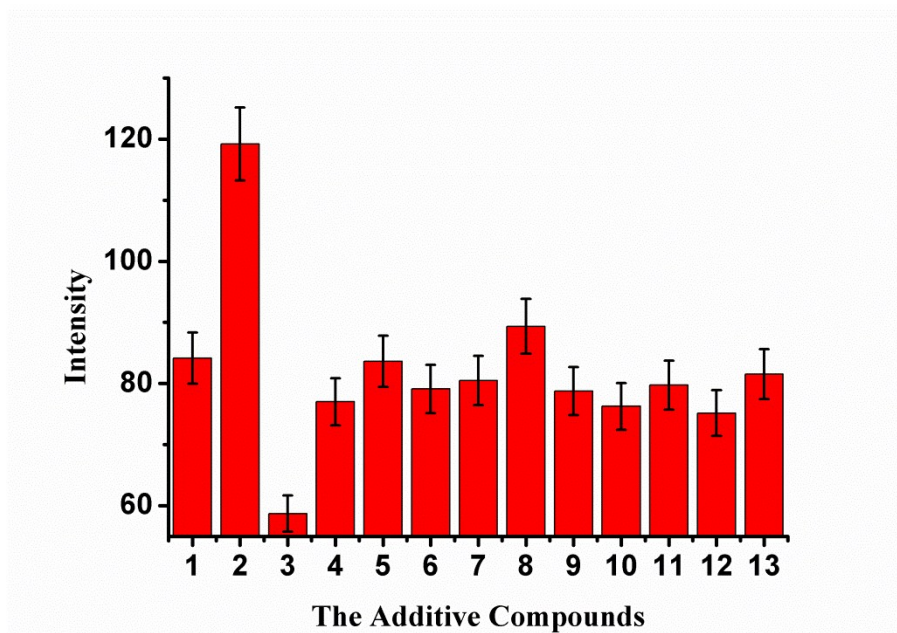


**Fig. S30.** The fluorescence emission spectra of **Ir-Es** ( $2 \times 10^{-5}$  M) mixed with different biomolecule (1, control; 2, CD-DNA; 3, PBR 322, 4, RNA; 5, L-Glutamic acid; 6, DL-Methionine; 7, Aspartic acid; 8, Leucine; 9, Tyrosine; 10, proline; 11, Tryptophan; 12, Serine; 13, L-Threonine).

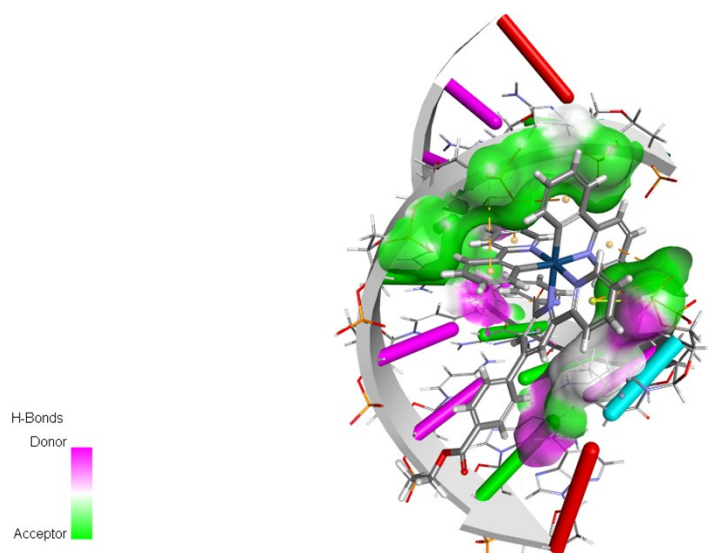


**Fig. S31.** The molecular docking models obtained from modeling the interaction between **Ir-Es** with DNA fragment.



**Fig. S32.** *In vivo* PDT extracted mouse solid tumor model after 21<sup>st</sup> days, treated with PBS, 660 nm light only, **Ir-Me** complex, *Ce6* and **Ir-Es** complex.

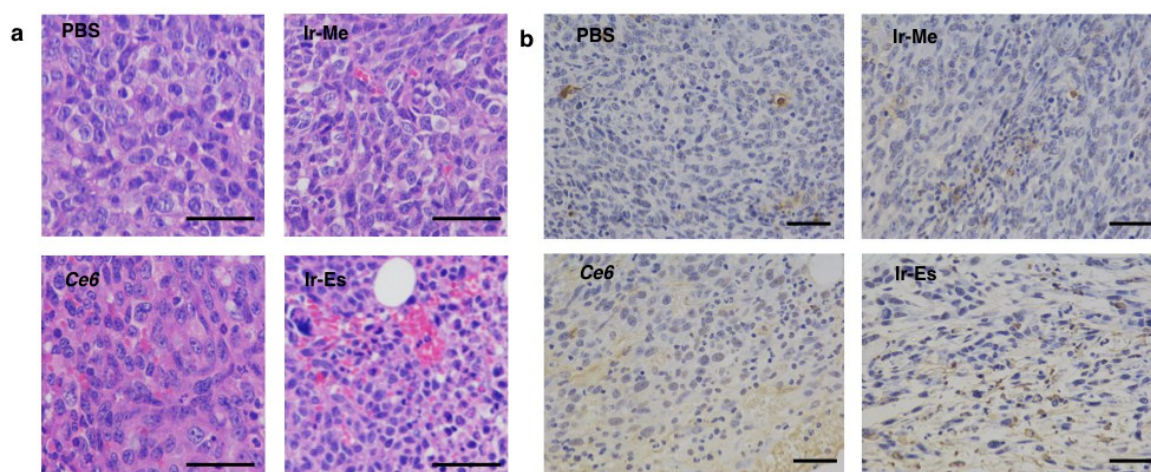


**Fig. S33.** (a) Tumours at 21<sup>st</sup> days post-treatment and corresponding H&E staining of tumour slides. (b). Tumours at 21<sup>st</sup> days post-treatment and corresponding TUNEL staining of tumour slides. Scale bars = 100  $\mu$ m.

## Reference:

- [1] J. V. Caspar, T. J. Meyer, *J. Am. Chem. Soc.* **1983**, *105*, 5583.
- [2] G.Y. Li, Q. Li, L. L. Sun, C. S. Feng, P. Y. Zhang, B. Yu, Y. Chen, Y. Wen, H. Wang, L. N. Ji, H. Chao, *Biomaterials*, **2015**, *53*, 285.
- [3] L. Au, Q. Zhang, C. M. Cobley, M. Gidding, A. G. Schwartz, J. Y. Chen, Y. N. Xia, *ACS nano*, **2009**, *4*, 35.
- [4] S. Yao, K. D. Belfield, *Eur. J. Org. Chem.* **2012**, *2012*, 3199.
- [5] B. Schmid, F. O. Garces, R. J. Watts, *Inorg. Chem.* **1994**, *33*, 9.
- [6] Costa R D, Ortí E, Bolink H J, et al. *Adv. Funct. Mater.* **2009**, *19*, 3456.